

Theoretical evaluation of continuous-wave time reversal acoustics in a
half-space environment

by

Blaine Harker

Submitted to Brigham Young University in partial fulfillment

of graduation requirements for University Honors

Department of Physics and Astronomy

Brigham Young University

May 2012

Advisor: Brian E. Anderson

Advisor: Kent L. Gee

Honors Representative: Roy W. Silcox

Signature: _____

Signature: _____

Signature: _____

ABSTRACT

Theoretical evaluation of continuous-wave time reversal acoustics in a half-space environment

Blaine Harker

Department of Physics and Astronomy

Bachelor of Science

Time reversal (TR) acoustics is a technique used to locate sources, using a set of transducers called a time reversal mirror (TRM) and is especially useful in reverberant environments. TR is commonly used to find acoustically small sources using a pulsed waveform. Here TR is applied to simple sources using steady-state waveforms using a straightforward, computational point source propagation theoretical model in a half-space environment. It is found that TR can effectively localize a simple source broadcasting a continuous wave, depending on the angular spacing. Furthermore, the aperture (angular coverage around the source) of the TRM is the most important parameter when creating a setup of receivers for imaging a source. This work quantifies how a TRM may be optimized when the source's location is known to be within a certain region of certainty.

ACKNOWLEDGMENTS

First of all, I owe a big thanks to one of my advisors, Dr. Anderson, for his willingness to assist as a long-distance advisor and see this project to its completion. He has been very helpful in every stage of the research over the past couple of years. Also, I'd like to thank Dr. Gee and Alan Wall for their help regarding my questions with the F-22 jet experiment. Thank you Acoustical Society of America and Office of Research and Creative Activities (ORCA) at Brigham Young University for funding this project. I am indebted to the BYU Acoustic Research Group for their facilities as well as the Fulton Supercomputing Lab for facilities and as well as help with generating my batch scripts. Finally, I'd like to thank my parents and grandparents who inspired me to work hard, dream big and to enjoy the journey.

Contents

Title and signature page	i
Abstract	ii
Acknowledgments	iii
Table of Contents	iv
List of Figures	vi
1 Introduction	1
1.1 Time Reversal: Basic Theory	1
1.2 Hypothesis	4
2 Methods	6
2.1 Model Design	6
2.2 Parameters of Study	8
2.3 Computer Simulations	12
2.4 Localization Quality Metric	13
3 Results and Analysis	16
3.1 Dependence on Angular Spacing	18
3.2 Dependence on Angular Aperture	22
3.3 Other Dependencies	26
3.3.1 Region of Certainty	26
3.3.2 Frequency	26
3.3.3 TRM Layout Shape	27
3.3.4 TRM Radius	27
3.3.5 Moving the Source Off-Center	28
4 Conclusions	30
A Applying Time Reversal to Military Jet Noise	33

B	MATLAB Code	36
B.1	Forward / Backward Propagation Step with Time Reversal	36
B.2	Parameter Iteration Testing	42
	Bibliography	57

List of Figures

1.1	Simple source and receiver model using time reversal	3
2.1	Forward propagation using a virtual source	7
2.2	Backward propagation individual pressure fields from arrival paths	9
2.3	Summed wave field of backward propagation step	10
2.4	Parameters of the TRM	11
2.5	Identifying the source location	13
2.6	Source to field ratio	15
3.1	Representative time reversal mirror setup	17
3.2	Comparison of real and absolute pressure fields	18
3.3	Backward propagation while varying the number of TRM Elements	19
3.4	Source to field ratio with varying angular spacing	20
3.5	Comparison with $\lambda/2$ TRM element spacing.	21
3.6	Varying the angular aperture of the TRM.	23
3.7	Comparison of various angular apertures	24
3.8	Normalized data comparing various angular apertures	25
3.9	Quality factor analysis for sources geometrically off-center the TRM	29
A.1	Evening test showing F-22 jet plume	34

Chapter 1

Introduction

Acoustic source localization methods are the subject on an ongoing field of study with a broad range of applications. One such method is time reversal (TR), a simple yet powerful technique for source localization in a complex environment. Fink, a well-regarded researcher in TR studies, provided general procedures and guidelines in this field, many which have set the standard.¹ One guideline considered in this thesis is the qualitative suggestion for array spacing for the transducers used. This introduction presents a brief overview of TR as well as the array spacing guideline suggested by Fink and a discussion regarding that guideline.

1.1 Time Reversal: Basic Theory

TR is a type of acoustic localization²⁻⁴ with many applications, such as lithotripsy to destroy kidney stones,⁵ earthquake localization and characterization,^{6,7} crack localization and characterization,^{8,9} target scatterer detection,^{10,11} land mine detection,¹² and secure underwater sound communication,¹³ though in some ways TR is still in the development stage. One of its fundamental uses is to localize a sound source of unknown location in a complex

environment.

The essence of TR may be described in terms of a simple analogy. Imagine a movie of a pebble dropped into a pond. Circular ripples spread out away from the drop location. If one were to play the movie backwards in time, the ripples would converge at the drop location, recreating the initial disturbance caused by the pebble. This is the essence of the TR technique. Imagine there are sensors that record these ripples on the water surface from an unknown source at various sensor locations, we then reverse the detected signals, and broadcast the reversed signals from the sensor locations. As a result, part of the waveform broadcast from each of the sensors will arrive simultaneously at the initial disturbance location such that the waves will interfere constructively and reproduce the pebble's initial agitation.⁴

This analogy extends easily to the idea of sound source localization. Fink explains that since the linear wave equation contains a second-order time derivative, if a source with a waveform $p(\mathbf{r}, t)$ solves this equation, then $p(\mathbf{r}, -t)$ will solve it as well.² Let us assume that an unknown source creates a signal that propagates to a receiver [see Fig. 1.1(a)]. Sound propagates spherically from the source, reflecting from the boundary so that two paths arrive at the receiver. If the receiver is omnidirectional, it records the waveform of each arriving signal, regardless of whether the signal comes directly from the source or via a reflective surface. Note that reflective surfaces create multiple propagation paths from source to receiver. The received signal is reversed and broadcast from the receiver location. In Fig. 1.1(b), each path is now traversed by both the direct and reflected signals, resulting in four arrivals at the original source location. The solid lines correspond to the original paths traveled and the dotted lines are the alternate paths taken by the direct or reflected signal. Without directional information, each waveform arrival will not only retrace its original path to result in constructive interference, but they will also trace other paths back

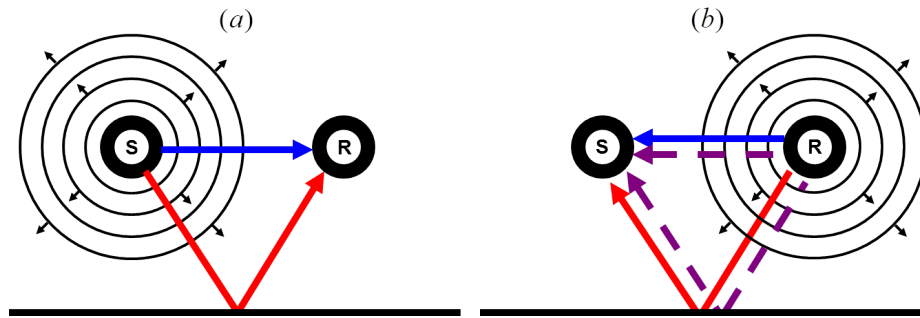


FIG. 1.1. Schematic drawing of the two steps of the time reversal process, (a) forward propagation and (b) backward propagation. This drawing helps illustrate the propagation paths in each stage.

to the source resulting in destructive interference. These additional paths are shown by the dotted lines. Fortunately, the constructive interference statistically creates a stronger response than does the destructive interference.

In the forward propagation step, the waveform recorded by a standard receiver receives no information as to the direction of incoming paths. Therefore, in the backward propagation the received waveform is simply reversed in time then broadcast from the receiver location. This results in a constructive focusing since the propagation paths are encoded in the timing of the forward propagation arrivals.

With the addition of multiple receivers, more information can be recorded from the source, and hence the backward propagation will yield a more precise and identifiable localization of the original source. If the sound source is a pulse, this localization results in localized spatial focusing and pulse-like temporal reconstruction. If the source is a continuous wave (CW), the localization may still be spatially focused but it may also require many transducers.¹⁴ The use of multiple transducers in the TR process constitutes an array known as the time reversal mirror (TRM).¹⁵

As long as the environmental conditions (e.g. sound speed profile and boundary conditions) are either known or the environment is stable, an accurate model can be created for

the backward propagation step and the transducers will broadcast their respective signals to retrace initial paths from the source to TRM.¹⁵ To summarize, when the TRM records an arriving signal, the signal is reversed, and subsequently broadcast, the result at the original source location (in addition to the background side lobe byproducts of TR) is to reproduce a reversed-in-time reproduction of the original sound.

TR provides advantages to alternative sound localization techniques but it also has its limitations. TR is simple in that it makes no assumptions about the sound source and it does not require complex algorithms or inputs (such as computed phase delays as in the case of beamforming techniques). Furthermore, while other sound localization methods break down with an increasingly complex environment, such as with a number of reflective surfaces, the efficiency of TR actually increases.² However, the medium of interest cannot change between the forward and backward steps of the TR process, or the medium must be accurately known if the backward propagation step is done computationally. In addition, TR requires simultaneous recordings for each transducer used in the setup, and the source localization is restricted to the diffraction limit¹⁵ (as are many localization methods). Finally, the spacing of transducers in the setup is an important factor, as grating lobes may be present in the field of interest (as is the case with most ray tracing techniques). The question of the appropriate transducer spacing in a TR experiment will be discussed in depth here.

1.2 Hypothesis

According to Fink *et al.*, spatial separation of TRM transducers by $\lambda/2$ (where λ represents the wavelength of the broadcast signal) is necessary to avoid grating lobes (also a general guideline in array design¹⁶), however they clarify that such spacing is not necessary if the

TRM is pre-focused on the source of interest.^{1,15,17} The present study will add further discussion to this guideline. In a realistic experiment it can quickly become impractical to use half wavelength spacing and a more economical and simple experimental design is desired. We optimize the number of transducers needed for a TR experiment given a relative knowledge of the source location and frequency content. In optimizing the TRM layout we find that TR can effectively localize a simple source broadcasting a CW, depending on the angular spacing. The results of this analysis can be used in further research to generalize TR reconstruction of more complicated sources.

In addition, there are many artifacts of TR that can affect the extent and quality to which the original source can be identified in the backward propagation step. Many of these parameters depend principally on the positioning and design of the TRM. The purpose of this thesis is to determine the dependency of these parameters on the quality of the TR focusing. We show that the aperture of the TRM is a primary parameter to consider when designing a TRM layout for imaging a source. Other parameters are influential as well and will be discussed in the following chapters. This feasibility study has been developed to apply specifically to jet noise (See Appendix A); however it has been generalized so that a similar experiment using steady state waves in a half-space environment may benefit from these results.

This analysis is directed towards developing useful guidelines in order to set up an effective recording of the forward propagation step in a TR experiment. Qualitative details regarding how many sensors to set up, where they should be placed, and frequency limitations for this setup are also addressed. To this end, we explore the efficiency and limitations of this technique due to the number of TRM sensors used, the angular coverage of the TRM, frequency, and an assumed *region of certainty* of the source location.

Chapter 2

Methods

2.1 Model Design

The present study uses a point source broadcasting a single frequency in a half-space environment. From a theoretical study using a single frequency, further complexity can be added using superposition of single sine wave sources that could in principle synthesize a more complex source. Although in many experiments a source (such a jet source) is complex and extended, the point source is used in these analyses because the focus is to optimize the sensor positions for a TRM layout. This provides a foundation for future work.

The source broadcasts a simple CW sine-wave omnidirectionally. The source is placed at a position $z_0 = 1.5\lambda$ above a hard surface, thus representing a source in a half-space environment. In order to represent the ground reflection in the model, the source at height z_0 was reflected about the ground plane to create a virtual source at height $-z_0$. The TRM elements would thus record the superposition of two sine waves, the direct signal from the source to each coplanar TRM element and the reflected path arrival depicted in Fig. 2.1(a).

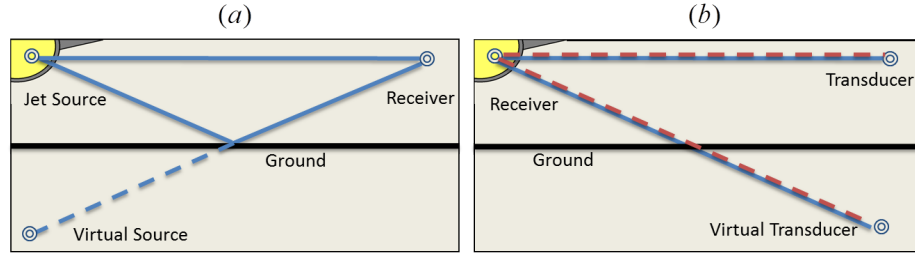


FIG. 2.1. Illustration of the arrival paths of (a) the forward propagation and (b) the backward propagation step. In (b), the direct arrival path from the forward propagation step is indicated by a solid line and the reflected arrival is indicated by a dashed line.

Then the equation for the field in the forward propagation, for a given wavenumber, k , and in the xy plane of the source, is

$$F_{fwd}(x, y, t) = \sum_{n=1}^N \frac{A}{r_d} e^{j(kr_d - \omega t)} + \frac{A}{r_r} e^{j(kr_r - \omega t)}, \quad (2.1)$$

where A is the amplitude, j is the unit imaginary number, ω is the angular frequency, and the vector r_d represents the distance from the source to the point (x, y) on the planar field and r_r is the path from the virtual source to (x, y) . N represents the number of elements in the TRM. A pressure field in the plane of the source and the TRM elements is created for every element within a given TRM and summed linearly.

In the backward propagation step, only the information received by the sensor elements can be utilized, so the individual fields from the source and virtual source are not separated. Therefore, only the combination of the amplitude and phase information from each signal is used in the backward propagation. We define θ_d and θ_r as the phase information from the direct signal and reflected signal respectively. Similarly we define A_d and A_r as the amplitude from each respective signal.

The backward propagation step requires that the medium have similar conditions to those of the forward propagation step.¹⁵ When each element transmits the reversed signal in the half-space, there will again be two paths of travel from the element to the original

source location from each arrival in the forward step. Thus, there will be four arrivals at the source location, two that interfere constructively and two that interfere destructively (See Fig. 2.1(b)). The backward propagation equation of the field in the plane of the source is

$$F_{back}(x,y,t) = \sum_{n=1}^N \frac{A_d}{r_{d,d}} e^{j(kr_{d,d}-\omega t+\theta_d)} + \frac{A_d}{r_{d,r}} e^{j(kr_{d,r}-\omega t+\theta_d)} + \frac{A_r}{r_{r,d}} e^{j(kr_{r,d}-\omega t+\theta_r)} + \frac{A_r}{r_{r,r}} e^{j(kr_{r,r}-\omega t+\theta_r)}, \quad (2.2)$$

where $r_{d,d}$ represents a direct arrival from the TRM element to point (x,y) on the plane and it was also a direct arrival in the forward propagation step. Similarly, $r_{d,r}$ is a reflection arrival to (x,y) and it was a direct arrival in the forward propagation step. This type of notation for $r_{d,d}$ and $r_{d,r}$ holds as well for $r_{r,d}$ and $r_{r,r}$. Note that the signals include no additional background noise and they were recorded assuming a steady state. The component fields for each of the four terms in the equation are shown in Fig. 2.2. The fields of Fig. 2.2(a) and Fig. 2.2(d) show a positive amplitude at the original source location (marked by arrows) and represent the signal arrivals that will add constructively in this region. The fields in Fig. 2.2(b) and Fig. 2.2(c) are the undesirable signal arrivals that interfere destructively at the source location. Once the individual fields for each element-source combination are calculated in the backward propagation step, they are summed together to obtain a total pressure field, seen in Fig. 2.3.

2.2 Parameters of Study

Several parameters are varied in order to gain further insight applicable in the design of a TRM layout (whose geometry is illustrated in Fig. 2.4). The parameters include the TRM element spacing, the TRM aperture, the region of certainty of the source location, frequency, shape and size of the TRM layout and the position of the source relative to the TRM geometric center. These parameters are described below.

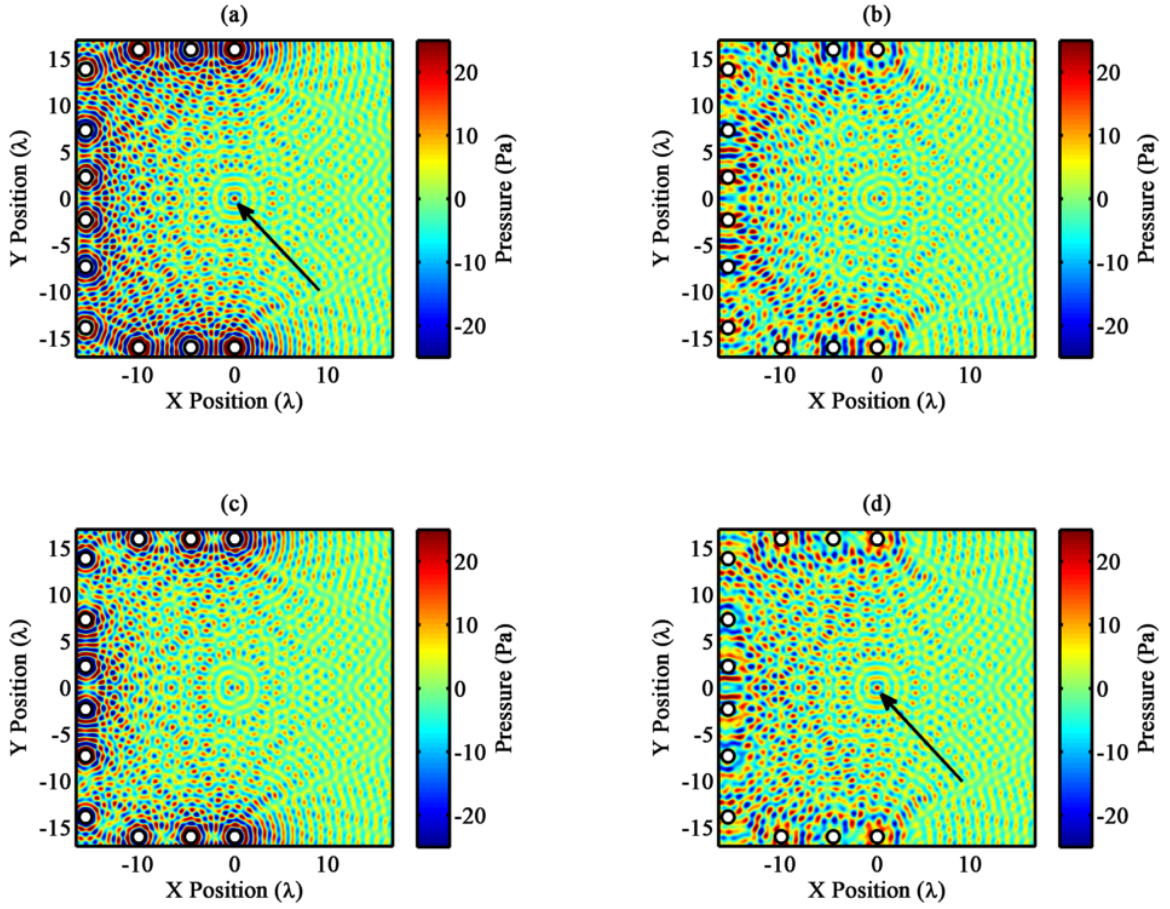


FIG. 2.2. The real part of the pressure wave fields created by each propagation path in the backward propagation step. The original paths from the forward propagation step and the arrivals paths are (a) the direct, direct path, (b) direct, reflected path, (c) reflected, direct path, and (d) reflected, reflected path [see Eq. (2.2)].

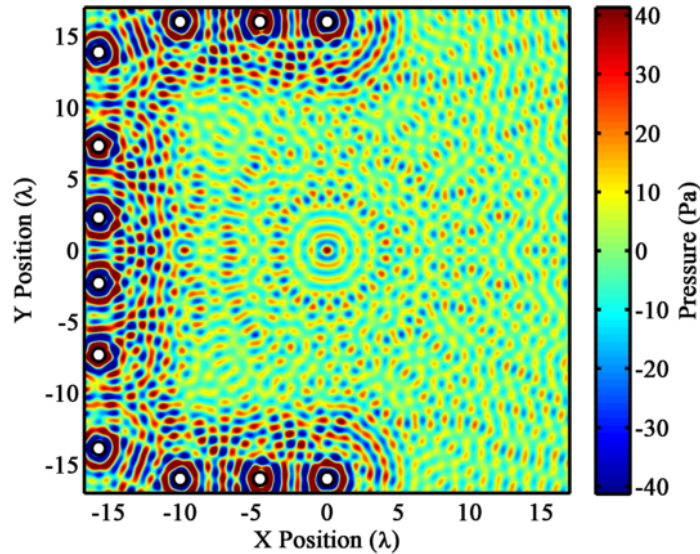


FIG. 2.3. The summed real part of the pressure field (from the fields in Fig. 2.2), which simulates the total backward propagation wave field.

The TRM *element spacing* is the distance between adjacent TRM elements. Half-wavelength spacing between elements is used to eliminate grating lobes globally. However, as will be shown later, for cases where the source is known to a certain extent this spacing may be relaxed considerably since grating lobes will not interfere with the region of interest. In this study, the element spacing was found to show unique properties associated with an angular separation rather than separation distance. Hence, the TRM elements were spaced at an equal angle about the source, even when the shape of the TRM was not circular. When the TRM layout was not circular, the distance between adjacent elements was varied but the angular spacing between elements was kept the same as for a circular TRM by projecting the element location along that angle. Thus the elements would not be equally spaced but they would be separated by an equal angle relative to the source location.

The *angular aperture* is the total angular span that the TRM spans around the source. The angular aperture may be varied anywhere between 0 to 2π radians about the source.

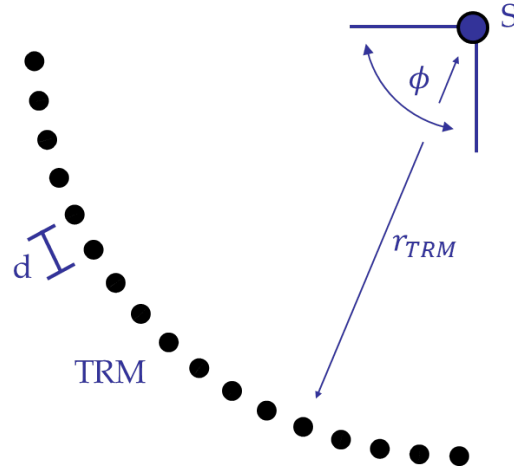


FIG. 2.4. Illustration of the geometry of the time reversal mirror layout with angular spacing d , time reversal mirror radius r_{TRM} , and aperture angle ϕ around source S .

Six different aperture sizes were used, varying from a small $\pi/12$ radian coverage to a full 2π radian coverage.

The *region of certainty* refers to the relative knowledge of the source position. This is defined by a square of a determined size which is centered upon the source location. In this study, a square with sides of length 5λ by 5λ was used. Notice that while the source location is identifiable in the center of Fig. 2.3, there are other artifacts in the field which make source localization more difficult and these artifacts would not be present if the elements were more tightly spaced. However, if the source location is known a priori to within 2.5λ , then the source location is easily recognizable in the backward propagation wave field. Altering the region of certainty affects the localization quality of TR as the field of interest about the source is changed. In practice, it is reasonable to assume some certainty of the location of the sound source.

The shape of the TRM used in the simulations traced out a circular shape or a square shape. As mentioned previously in the case of the square array, the elements were spaced at an equal angle from the source and not at a constant separation distance.

Finally, it is noteworthy to mention that when the position of the source was moved off of the geometric center of the TRM, that the angular spacing of the TRM elements and the aperture were not altered. However, the *effective* angular spacing and aperture would change as a consequence of the source being moved at a position off-center of the TRM layout. The results of each parameterization study are given in Chapter 3.

2.3 Computer Simulations

Using the simplified model described here, parameters are quickly varied, iterated and retested, producing results for hundreds of different scenarios. In this manner, the model allowed for a pressure field simulation over a large area around the source location. It also allowed for a large number of parameters to be studied. The script developed for this parameterization study allowed for multiple tests in a very small amount of time. Additionally, many of the tests were combined to utilize available RAM and run efficiently over multiple processors simultaneously. One such consideration was in utilizing MATLAB's matrix multiply capability and other functions which are designed for multiple processor use. This decreased overall computation time significantly. Tests were conducted on the BYU Acoustic Research Group's Kirchhoff Server, a Dell T Series Tower Server with an Intel® Xeon® E5530 with 2 processors for a total of 16 threads, and 48GB of installed RAM. Furthermore, BYU's Mary Lou 6 (M6) was also used. The Mary Lou 6 is a supercomputer with over 500 nodes and each node consists of 12 Hex-core Intel Westmere processors and 24GB of utilizable RAM. Because of restrictions associated with using MATLAB, only one node on the supercomputer could be utilized per job. However, multiple jobs could be submitted on the M6. Thus, scripts were converted to batch jobs which could be submitted simultaneously to the supercomputer. A general sampling of the scripts

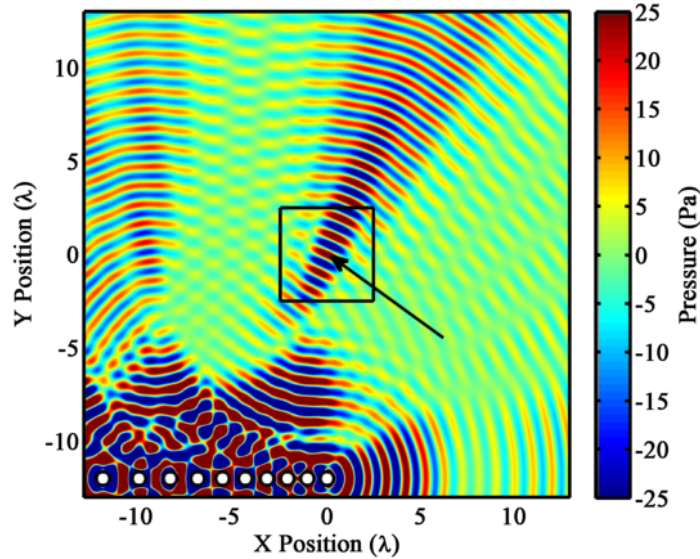


FIG. 2.5. Backward propagation wave field of a time reversal mirror using a partial square layout of aperture $\pi/4$ radians and 10 TRM elements. The arrow points to the original source location and the black outline a particular region of certainty ($5\lambda \times 5\lambda$).

is included in Appendix B.

2.4 Localization Quality Metric

While the source location of Figure 2.3 was easily identifiable, other situations such as that shown in Figure 2.5 are not as simple. In this case, the beaming from the small aperture results in a poor localization of the source. Optimizing the time reversal mirror requires that there be some type of methodology in determining the position of the source and the certainty that it is indeed the original source location. A metric was developed in order to quantify the quality of localization, the source to field ratio (SFR). This metric is useful not only in its ability to compare quality of localization as a single parameter is varied, but it also allows for a comparison across many parameters and their effects on the quality.

In the reversal and backward propagation of the waveforms from the received locations,

a high amplitude pressure is created at or near the point where the original source was located. The SFR measures the pressure amplitude at the point that the source was originally located and compares this to the average of the amplitude surrounding this location as

$$\text{SFR} = \frac{|F_{0,0}|}{\frac{1}{K} \sum_{i,j} |F_{i,j}|}. \quad (2.3)$$

In this equation, $F_{i,j}$ is the pressure at a given point of the field, the source is located at the origin $(0,0)$, and K is the number of field points within the field to be averaged. The field points are taken from $\lambda/4 \leq |x(i), y(j)| \leq 5\lambda/2$ for the case of a local field to be averaged with 5λ by 5λ sides. The field points are not taken for $|x(i), y(j)| \leq \lambda/4$ so as to not mix the source pressure location with the surrounding field and detract from the SFR. A high SFR suggests a strong focusing of energy, thus allowing localization. An example of this source and field is shown in Fig. 2.6. The TRM includes ten elements with total aperture π radians and an inter-element spacing (measured by angle) of $\pi/9$ radians. The TRM of Fig. 2.5 is only $\pi/4$ radians with an inter-element spacing of $\pi/36$ radians. In Fig. 2.6, the pressure at the source location is compared with the average value of the nearby field, or region of certainty. Applying equation 2.3 in this example, the SFR is 3.91, whereas the SFR for Fig. 2.5 is only 2.64.

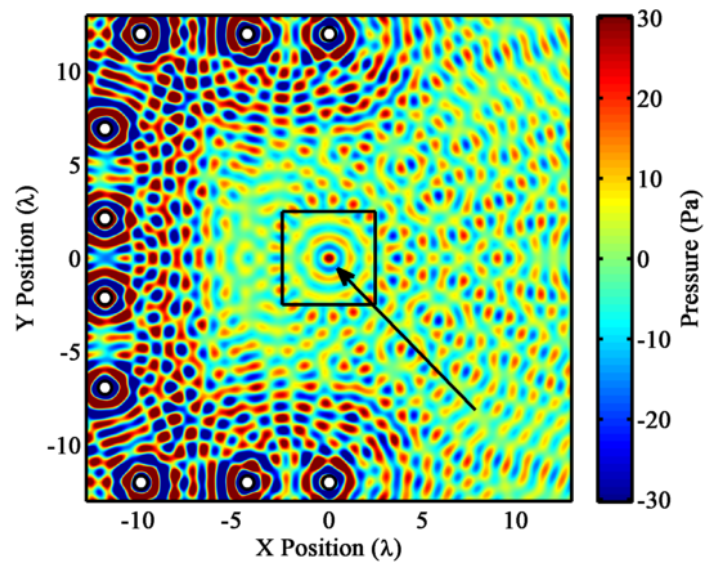


FIG. 2.6. Backward propagation wave field of time reversal mirror showing the source location (marked by the arrow) and region of certainty ($5\lambda \times 5\lambda$ black outline).

Chapter 3

Results and Analysis

This chapter is divided into sections for each parameter which was optimized in the study. It is organized in order of importance to the TRM setup for optimization and qualitative results. A few of the more important parameters to be discussed are the dependence of the SFR on the angular spacing and the angular aperture of the TRM. The *region of certainty*, frequency, shape and size of the TRM, and position of the source are also discussed.

According to prevailing theory and practice, half-wavelength spacing of TRM elements is necessary to avoid grating lobes, although this restriction can be relaxed if the source is pre-focused on the source.^{1,15,17} There has been little or no discussion to quantify the extent to which the element separation distance may be increased. We assume that the source location is known to within a certain region. Results will be given for the case when the TRM layout is centered around the source, then in Section 3.3 results will be discussed which generalize our findings to a source which is moved off-center of the TRM layout.

Shown in Fig. 3.1(a) is a simple TRM centered about a simple source in a homogeneous half-space environment which broadcasts a continuous sine-wave in the forward propagation step. This is a general example of the setup used in the study. The TRM and source are coplanar, that is above, and parallel to the ground which is located in the xy plane,

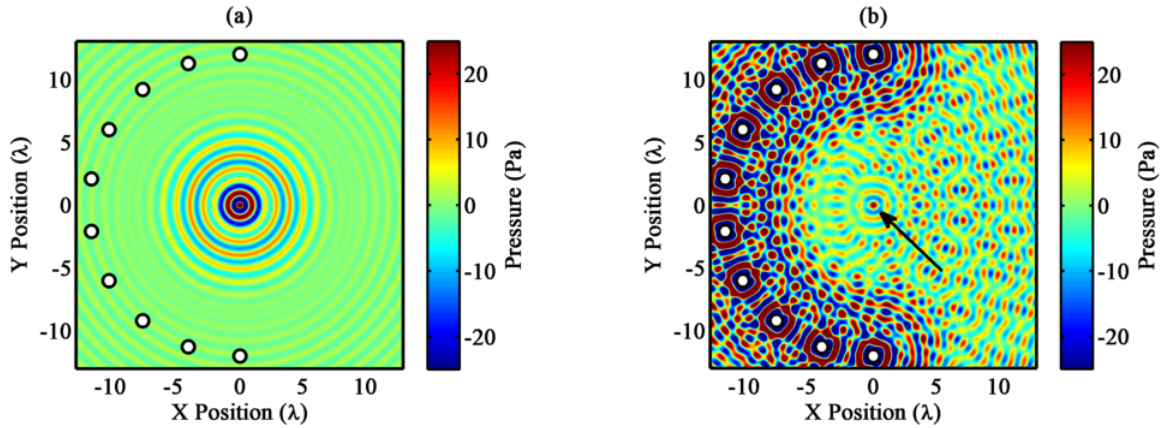


FIG. 3.1. Representative pressure wave fields from a time reversal computational model using 10 transducers for (a) the forward propagation and (b) the backward propagation step.

thus the wave field includes interference due to the ground reflection. The mirror elements (shown as white dots in the pressure field) record information received directly from the source as well as the reflection paths off the ground boundary. Note the interference null in the field at 6.9λ radius around the source where the direct and reflected wave fields cancel one another. In Fig. 3.1(b), the waveforms received are reversed in time and broadcast. In addition to other uncorrelated artifacts, this creates a localized pressure maxima at the location of the original source as shown by the red dot and the arrow. Ignoring the region near the TRM where the wave field is at higher amplitudes, the source location in this plot is the point of maximum pressure amplitude.

The pressure magnitude of the back propagation field is utilized for analysis instead of the real part of the pressure. This has advantage in pointing out features of the field without regard to the $e^{j\omega t}$ time dependence. An example of this advantage is shown in Fig. 3.2. Figure 3.2(a) shows the real part of the pressure wave field (see Eq. (2.2)) for the backward propagation step and Fig. 3.2(b) shows the pressure magnitude. In Fig. 3.2(b), the original source location is visibly more identifiable. Furthermore, the magnitude of the pressure at a particular field location is typically more desirable from experimental data.

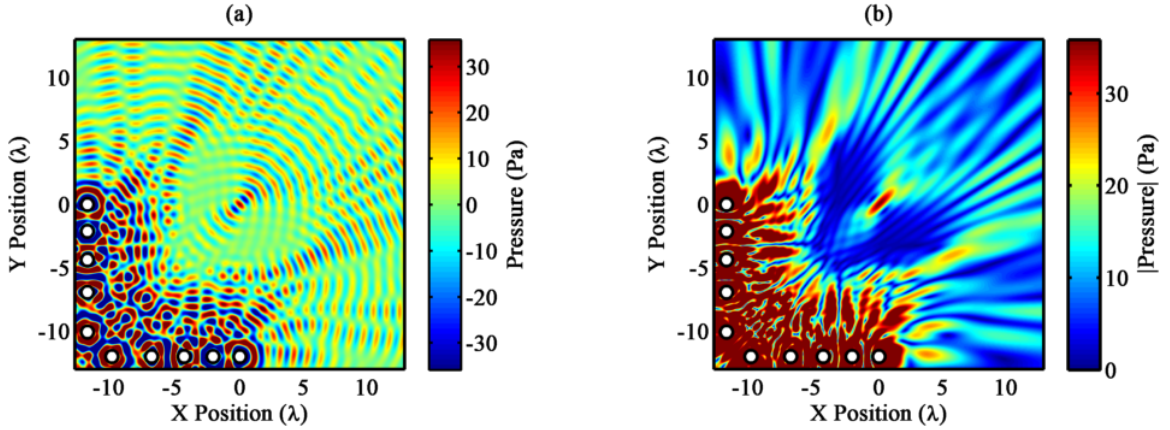


FIG. 3.2. Spatial maps of (a) the real part and (b) the magnitude of the pressure wave field from a sample time reversal model.

3.1 Dependence on Angular Spacing

Fink described the spacing of TRM elements as being a primary contributor to the quality of source localization.¹ Thus the main focus of this computational study was the qualification and further study of the dependency of the element spacing in the TRM to the SFR. As seen in Fig. 3.3, the backward propagation fields are plotted when three different TRM layout densities are used in similar conditions while the total angular aperture is kept constant. In this case, a circular TRM layout of radius 12λ centered about the source is used. The TRM elements are evenly distributed about a 2π radian circle surrounding the source. The region of certainty is a square with $5\lambda \times 5\lambda$ sides that is centered about the original source location. As the number of elements in the TRM increases, the field surrounding the immediate vicinity of the source location decreases in amplitude, increasing the localization quality. This effect is seen in Fig. 3.3. As additional TRM elements are used, the area of decreased amplitude surrounding the source increases. Once this area encompasses the region of certainty, the SFR arrives at a limiting value. The SFR for the cases shown in Fig. 3.3 are (a) 3.88, (b) 6.12, (c) 6.34, and (d) 6.34.

It was found that, in general, as the angular density of elements was increased, the

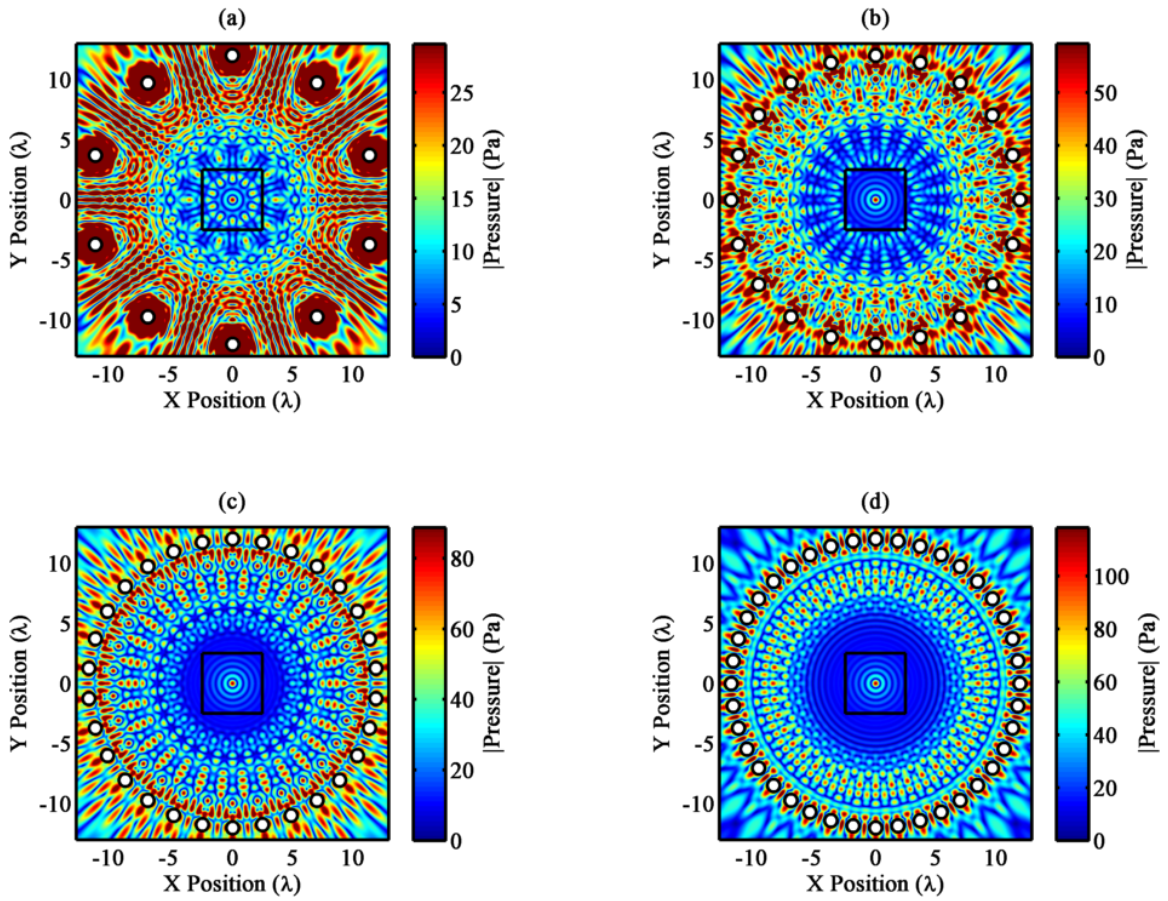


FIG. 3.3. The backward propagation wave fields for a time reversal mirror of (a) 10 elements, (b) 20 elements, (c) 30 elements, and (d) 40 elements.

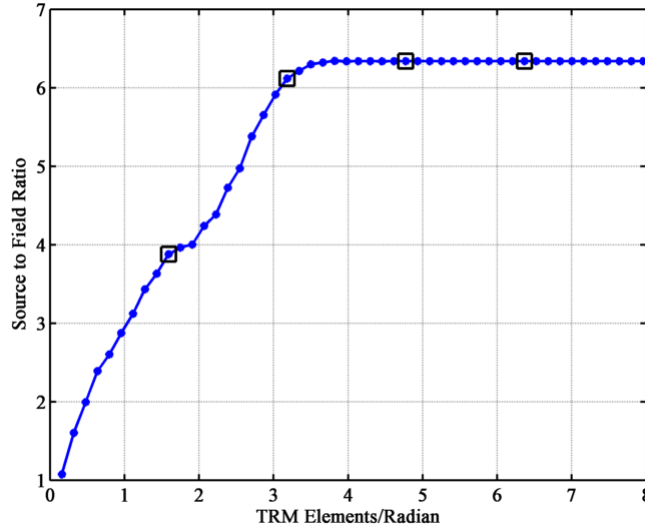


FIG. 3.4. Source to field ratio of for a time reversal mirror with a variable number of time reversal mirror elements given a set angular aperture vs. the number of mirror elements per radian. The TRM layout for the data shown is circular in shape and has a total angular aperture of 2π radians. The source to field ratio of the plots in Fig. 3.3 correspond to the box marker values.

quality of the localization increased up until it would reach a limiting value, irrespective of the shape of the TRM or the total angular coverage. Shown in Fig. 3.4 is the source to field ratio as a function of the TRM element spacing. Notice that for this particular set of models, a sufficient linear density of elements to optimize the SFR are approximately 3.5 elements per radian. Beyond this value, additional TRM elements do not increase the SFR for the given region of interest. This means that the optimal element spacing is about 3.4λ . An equivalent mirror with $\lambda/2$ spacing between each element would require 7 times as many TRM elements. In general, for a source centered on the TRM in the aforementioned conditions, the peak value of the SFR would require significantly fewer TRM elements than if a half-wavelength spacing criteria were used. This peak value, and the number of TRM elements sufficient to attain it, is affected by other parameters as discussed in the following sections.

We now show an additional example of a TRM that also does not require an angular

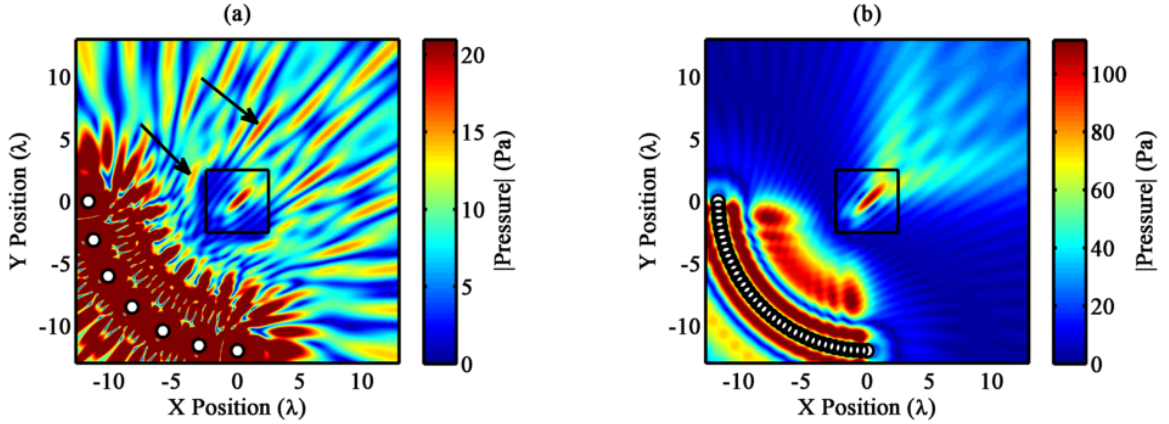


FIG. 3.5. Pressure magnitude spatial maps for a time reversal mirror with (a) 7 elements and (b) 37 elements. The time reversal mirrors have an angular aperture of $\pi/2$ radians.

spacing of $\lambda/2$. Figure 3.5 shows the backward propagation fields of a circular TRM layout with an angular aperture of $\pi/2$ radians. In Fig. 3.5(a), the element spacing is approximately 3λ and there are visible grating lobes type artifacts, some of which are identified by the arrows in the figure. Figure 3.5(b) shows the case where elements are spaced $\lambda/2$, there are no grating lobes, and the source location is easily discernible. However, note that both figures have similar fields within the region of certainty (denoted by the black box). Thus if the source location is known to within this region of certainty, a significantly fewer number of TRM elements is necessary in reconstructing the source location. A defined region of certainty of the source location will usually result in a significantly fewer number of TRM elements necessary to localize the source.

However, if the general source location is unknown, i.e. there is no region of certainty defined, then grating lobes result in features sufficiently similar to the true source localization as to prohibit proper source localization. This can be solved without the need of $\lambda/2$ element spacing through a larger angular aperture ($\geq 180^\circ$ may be needed) as discussed in the following section. A large angular aperture refines the localization from a beam-like localization to a more point-like region. The original source location and other artifacts

will be more point like in appearance. From this, an increased number of TRM elements will refine the wave field in the backward propagation step until the original source location is clearly identifiable. Geometric patterns also may aid in identifying the original source location as seen in Fig. 3.3, since features due to the grating lobes are symmetric about the original source location.

3.2 Dependence on Angular Aperture

The total aperture, or the angle which the TRM elements sweep out about the source, is often limited for practical purposes and we investigate here the effects that aperture would have on localization. In Fig. 3.6, an example is shown of different TRM layouts where the angular spacing is held constant and the aperture of the TRM is changed from $\pi/4$ radians to 2π radians about the source. As Fink *et al.* explains, the point spread function of the source localization is related to the angular aperture of the TRM.¹⁵ As the angular aperture is increased, the localization becomes better resolved until the point spread function reaches the classical $\lambda/2$ diffraction limit.² In Fig. 3.6(a) the source location is more difficult to resolve due to the other artifacts in the wave field. In the low angular aperture regime, grating lobes are visible and symmetric about an axis from the TRM to the original source location. These make identification of the source difficult, however if these lobes are outside of the region of certainty the lobes do not impede the source localization. In the high aperture regime, as seen in Figs. 3.6(c) and 3.6(d), the source is visibly distinguishable and the classical diffraction limit of the source localization is the limiting factor. For the cases in Fig. 3.6(a-d) the SFR values are 2.13, 2.74, 3.61, and 4.97 respectively.

This limiting resolvability of the point spread function is also apparent in the SFR for

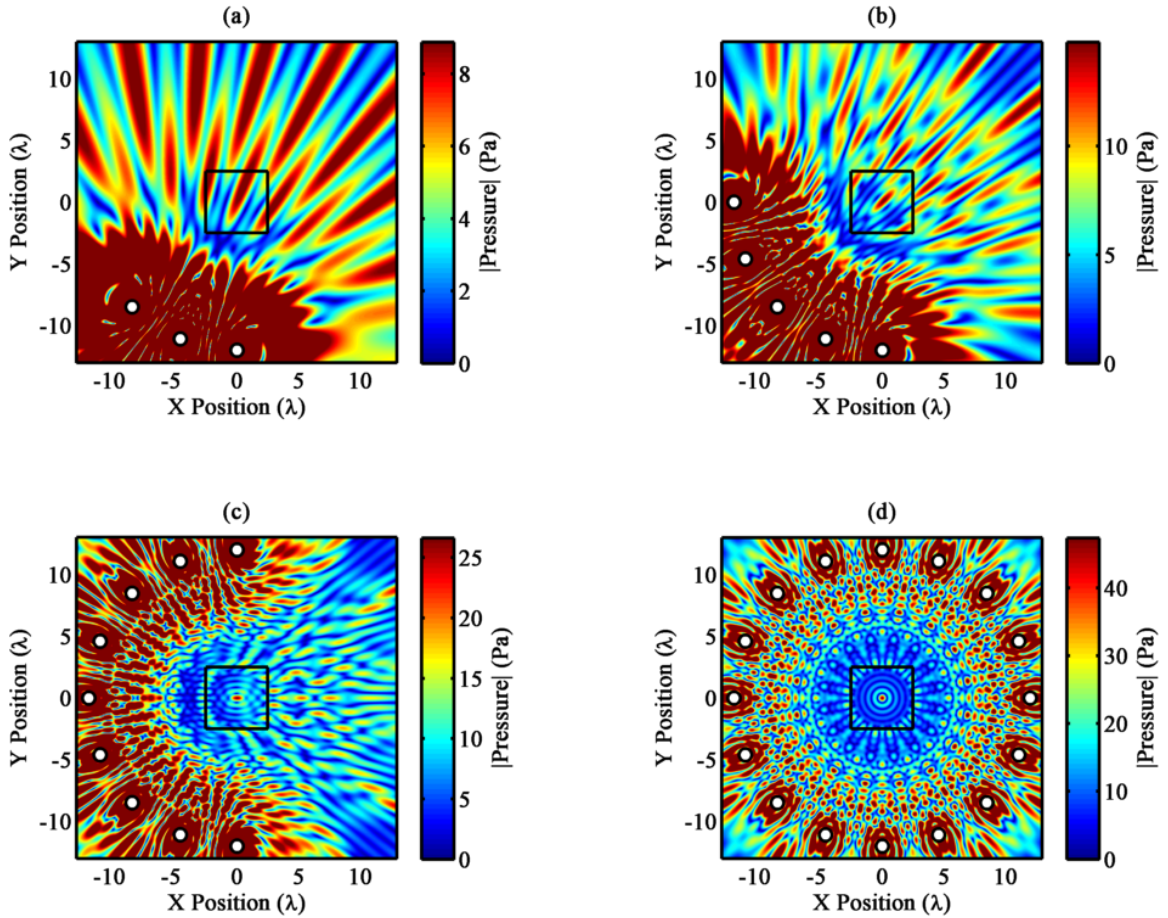


FIG. 3.6. Holding the angular spacing of TRM elements constant (2.55 time reversal mirror elements per radian), the aperture of the TRM is varied by (a) $\pi/4$ radians, (b) $\pi/2$ radians, (c) π radians and (d) 2π radians.

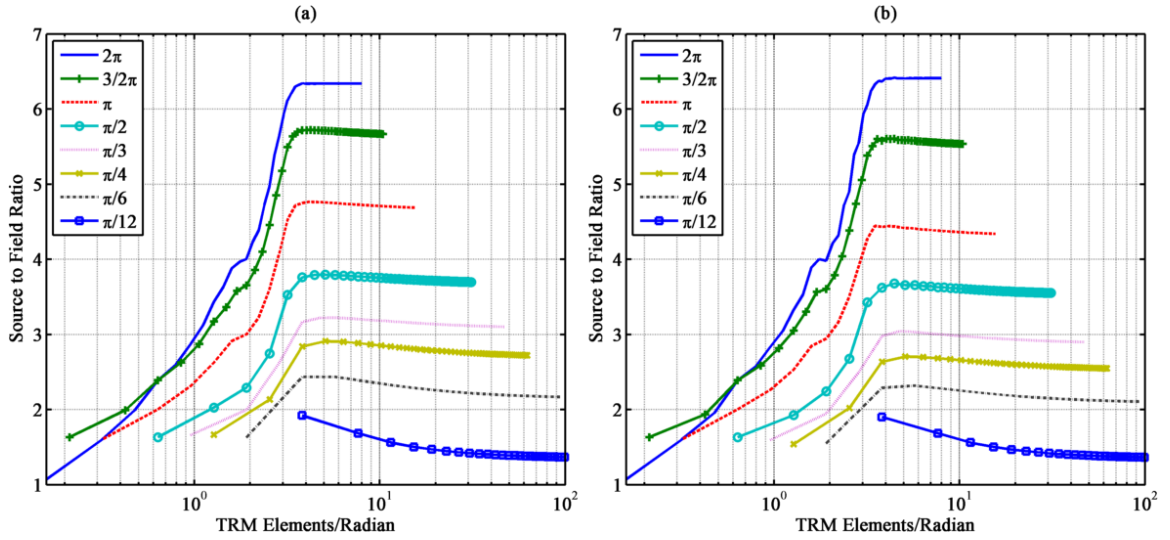


FIG. 3.7. Source to field ratio versus the number of mirror elements per radian for several different total angular coverages using (a) a circular time reversal mirror layout and (b) a square time reversal mirror layout.

these cases. Shown in Fig. 3.7 is a comparison of different TRM layouts with different total angular apertures while also varying the TRM element spacing for each fixed total aperture. As an example, the plots in Fig. 3.3, which each have a total aperture of 2π radians, correspond to the box marker values in Fig. 3.4, and the data from Fig. 3.4 may be seen in the blue solid line in Fig. 3.7(a). Figure 3.7(a) shows the results for circular TRM apertures while Fig. 3.7(b) shows the results for TRM layouts where the elements are arrayed in a square shape (the TRM shapes will be discussed in Section 3.3.3). If the total angular aperture is increased, there is a reduction in the point spread function near the source which yields a higher SFR. This general increase in resolvability of the source location due to an increased aperture was noted by O'Brien *et al.*⁷ and Larmat *et al.*¹⁸

Of particular interest is the limiting value of the SFR in each trial. If the curves of Fig. 3.7 are normalized to their respective peaks as shown in Fig. 3.8, the optimal TRM spacing for each aperture is only minimally affected. The similar trend of each aperture suggests only a minimal dependence between the angular spacing of the elements and the

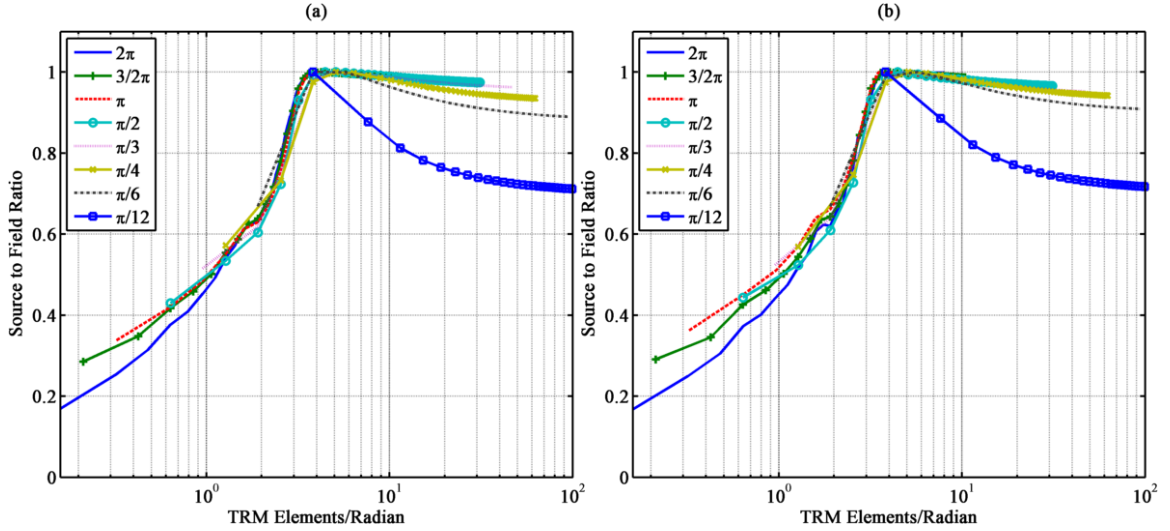


FIG. 3.8. Data from Fig. 3.7 which is normalized by the maximum source to field ratio of each set of data for (a) a circular time reversal mirror layout and (b) a square time reversal mirror layout.

angular aperture. As seen in Fig. 3.8, the value at which the SFR approaches a peak value is independent of the total aperture angle. For smaller aperture sizes, the effect of beaming in the direction of the source for TRMs of smaller total aperture does not necessarily result in a maximum pressure in the region of certainty, let alone at the actual source location (See Fig. 3.6(a)). Thus, in the lower limit of the aperture, the quality of localization does not increase with an increase in the angular spacing for small angular aperture TRMs (See Fig. 3.8) since the source region is not centered on the original source location. Therefore, a lower bound to the TRM aperture exists, dependent on the size of the region of certainty. We conclude that an increased total aperture angle, with fixed angular spacing between elements, increases the SFR resulting from a more optimal point spread function for the source reconstruction. Furthermore, given a region of certainty, in optimizing the peak value of each aperture we find that there is a fixed optimal spacing irrespective of the total aperture size for the TRM.

3.3 Other Dependencies

Further studies were done using other parameters that are taken into consideration when creating a TRM setup. These include the relative knowledge of the source location, the frequency of interest, the shape and size of the TRM layout, and the degree to which the TRM is centered on the source location. The following sections describe the effects each has in optimizing the TRM setup.

3.3.1 Region of Certainty

It has been found that when the area in which source is known to exist is increased (less certainty of the source location), the optimal number of TRM elements at which the peak SFR is reached increases proportionally. This shows a direct relationship between the knowledge of the source location and the necessary TRM element spacing. Stated another way, a better a priori knowledge of the location of the source directly corresponds to a reduced number of elements needed in order to optimize a given TRM layout.

3.3.2 Frequency

Given a TRM layout and a determined optimal angular spacing of TRM elements for a respective region of certainty, if the frequency of the source is decreased, there will also be a proportionate decrease in the optimal number of TRM elements required at which the quality of localization reaches a peak value. If the frequency of interest is increased, the TRM is optimized by either using additional elements or by gaining a better certainty of where the source is located. Thus for a certain TRM layout, there exists an upper cutoff frequency, above which the TRM element spacing is not optimal.

3.3.3 TRM Layout Shape

Different TRM layouts were tested to determine what effect each would have on the aforementioned results. Shown in Fig. 3.7(a) are the results of a parameterization study for circular layouts where each element is equally spaced and placed equidistantly from the source. In Fig. 3.7(b), each data set represents a square shaped mirror of a particular aperture size for the case that the angular aperture is 2π radians, or if it is a smaller aperture, the shape is a partial aperture of a square. The elements were equally spaced in terms of arc angle coverage, so that each part of the square shape had the same density of elements per unit angle. This allowed better comparison to the circular shaped layouts. In both cases, the optimal angular spacing of the elements is similar to one another, the circular shapes outperforming the square shapes by only an average of 3.5% for their respective peak values. As can be seen, there is some variation between the shapes, however the value where the quality factor is optimized remains the same. Thus the shape of the TRM layout does not appear to be very important.

3.3.4 TRM Radius

The TRM radius is the distance from a circular arc TRM to its geometric center. In the case of a square TRM layout, the TRM radius is defined as the distance from the square's center to its closest edge. As the radius of the TRM is varied, there was very little change in localization quality. For this reason, it is impractical to specify an optimal element spacing when optimizing the TRM layout for an experiment, since an element spacing when the mirror is one meter from the source will be ten times smaller than if the mirror is ten meters from the source, and this results in no change in the localization quality. Instead the number of elements per radian or angular density is found to be more useful for an optimization specification.

3.3.5 Moving the Source Off-Center

All previous results are determined for a source which is geometrically centered within the TRM. Cases where the source is moved off-center of the mirror are also considered. If the source is moved off-center from the TRM, the SFR varies with the apparent change in the angular aperture relative to the source position. If moving the source increases the angular aperture, the SFR increases. However, small deviations in the source position result in little effect on the optimal angular spacing of the elements. Shown in Fig. 3.9 are circular and square TRM layouts with an angular aperture of $\pi/2$ radians in 3.9(a) and 3.9(b) respectively, and π radians in 3.9(c) and 3.9(d) respectively. The figure depicts the resulting SFR when the source is moved from off center to various locations while the positions of TRM elements are fixed. Each value at different locations in the field represents the SFR for the field near the source at that location. The SFR increases as the source is moved closer to the mirror, which corresponds to an increased angular aperture. However, as the source continues to approach the mirror, the quality decreases as the high amplitude in the nearfield of each element relative to the desired focusing distorts the SFR.

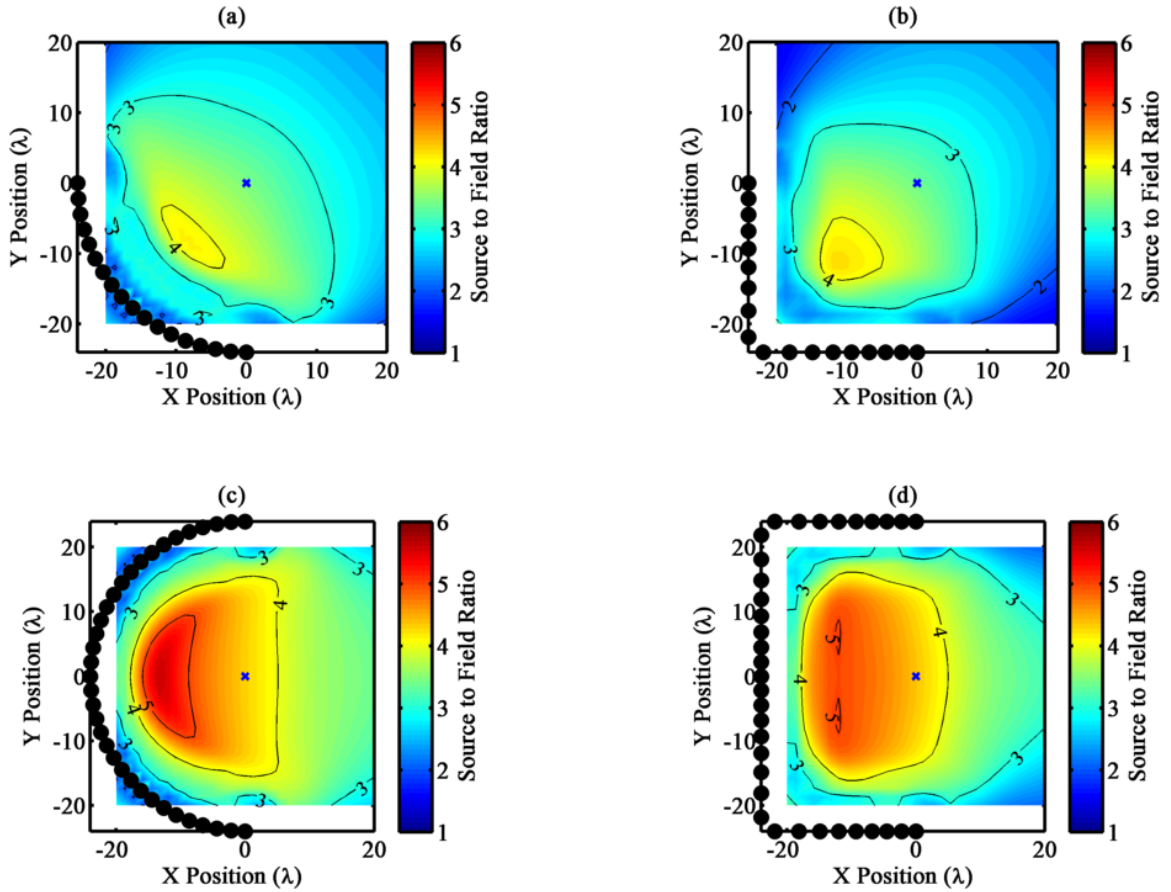


FIG. 3.9. Spatial maps of the source to field ratio when the source location is geometrically off-center of the time reversal mirror for (a) a circular time reversal mirror with $\pi/2$ radian aperture, (b) a square time reversal mirror with $\pi/2$ radian aperture, (c) a circular time reversal mirror with π radian aperture and (d) a square time reversal mirror with π radian aperture.

Chapter 4

Conclusions

In optimizing the layout of the TRM for a time reversal experiment it is found empirically that for a simple source emitting a CW signal in a half-space environment, the localization quality depends on the angular density of the TRM and the region of certainty. There is a peak localization quality value (SFR) that, depending on the relative knowledge of the source location (region of certainty), generally allows for relaxed conditions on the half-wavelength element spacing criteria suggested by Fink *et al*¹⁵ and others. Furthermore, optimization of the TRM layout is dependent on an angular density of TRM elements with respect to the source location rather than an absolute distance. Grating lobes, which cause other artifacts in the wave-field and hinder proper source localization can be ignored to an extent, provided the source is within a region of certainty. We have shown that the angular spacing of elements is the most important parameter given a fixed angular aperture on the TRM.

By increasing the angular aperture for a given TRM element spacing, one will increase the SFR thus allowing more accurate localization, however this requires that the total number of elements be increased. In this manner, the angular density of the element spacing is preserved. An increased aperture has little effect of the optimal angular spacing of elements

for an assumed region of certainty, except that an increased aperture reduces beaming effects that make the source location more difficult to identify since there is no temporally compressed reconstruction for a CW source as observed for TR experiments with pulsed sources.

Other parameters also contribute to the optimization of a TRM layout. As the region of certainty (i.e. relative knowledge of the source location) decreases in area, the angular density of TRM elements necessary to reach a peak SFR decreases proportionally. The frequency of the simple source is proportional to the number of TRM elements needed in a TRM layout to reach a peak SFR value. The shape of the TRM layout is only important inasmuch as it affects the angular density of the TRM elements. The TRM radius, or distance from the TRM layout to its geometric center, can be disregarded for idealized conditions (ignoring atmospheric absorption and signal to noise considerations for example) so long as the source does not lie within the nearfield of the TRM elements or at a null location in the field from direct and reflected interference of the source radiation. Finally, if the source is moved off of the geometric center of the TRM, the SFR is dependent on the TRM aperture relative to the new source location and whether the source is in a location where source reconstruction is more difficult. This may be a concern if the source is in the nearfield of the TRM elements or if the source is in a region of destructive interference caused by the ground reflection.

Further studies may be performed to increase understanding in applying TR to jet noise sources and other similar studies. This includes studying TR with an extended source,¹⁹ understanding the effects on the TR process with a temperature gradient in the source region, and understanding the effects that non-linear propagation has on TR for jet noise sources, though some work has been done in this area for a different application.^{20,21} With a better understanding regarding an optimized TRM layout, future experiments can be planned

for increased efficiency. This allows for more effective use of the elements in any given experiment, be it jet noise or any similar half-space application.

Appendix A

Applying Time Reversal to Military Jet Noise

Military jet noise research is active in developing the understanding of how the jet engine and turbulence create and propagate sound. The near-field acoustic radiation and the source characteristics of military jet noise are not well understood. Because of this, various research approaches utilize different methods to gain new insight with each new approach. Theories on the nature of the sources of jet noise continue to be developed,²² thus fundamental imaging studies increase knowledge which allows for a better engineering decisions in propulsion systems as well as safety guidelines for flight deck workers.

Jet noise is also an ever increasing concern for aircraft workers, airport communities and military personnel. During the 2010 fiscal year, over 1.4 million veterans received compensation due to hearing related damages while acting in service duties. While data are not limited to jet noise, it remains a primary culprit for hearing related damages, including tinnitus and hearing loss, which are the most prevalent service-connected disability for veterans.²³ This is an ongoing problem as the US military continues to anticipate for



FIG. A.1. Photograph of an F-22 Raptor held on the ground for acoustics testing.

permanent hearing damage of flight deck workers on aircraft carriers. Moreover, communities adjacent to airfields are constantly bombarded with the high intensity sounds from takeoffs. Increased sound levels from these aircraft can lead to declining real estate values.²⁴

One of the challenges in this study is in dealing with a complex sound source which creates non-linear sound waves and has varying degrees of coherence. Because of this, many researchers have used different methods to analyze the data and better understand the sound source.^{25–27}

Until now, there has been little research into the applicability of TR to jet noise. However, TR may prove to be effective in problems where beamforming and other ray-tracing techniques have limitations. A simple example and benchmark upon which other beamforming methods are compared is the delay-and-sum (DAS) method.^{28,29} Here, the arrival times or phase information of array transducers are compared and from that the arrival signals are phased accordingly to propagate a beamed wave field in the direction of the source.

Even the simplest beamforming method however requires phasing calculations that TR can reproduce intrinsically. Beamforming techniques are also inhibited by reflective surfaces, while, as long as the environment is known, TR benefits from these reflections.

There are many limitations to the TR method however when working with jet noise. TR has historically found its use when dealing with transient signals since the TRM has the potential of spatially and temporally locating a source. Jet noise, although turbulent in nature, is more akin to a long duration source, whereby the source's time of emission is lost when using TR. Furthermore, a jet noise source is complicated in that it is best described as an extended source, and noise radiated has important finite amplitude propagation characteristics.^{22,30} Temperature gradients in the propagation field are also an important consideration. Traditional methods of collecting jet noise data create further problems. Jet noise is usually recorded as the jet is on a hard surface in a half space, using an array which only partially surrounds the source. The temperature and size of the jet plume require that transducers recording the waveform be placed at a suitable distance from the plume and there are a limited number of microphones which record the waveform simultaneously.

With these considerations in mind, the purpose of this study is to gain a better understanding of the limitations and capabilities of TR in a perfectly rigid, half space environment using single frequency continuous waveforms with application to jet noise. As the potential of the method is realized, the development of useful procedures and techniques for utilizing TR with a jet noise source is possible.

Appendix B

MATLAB Code

B.1 Forward / Backward Propagation Step with Time Reversal

This code was used in the generation of most of the figures in the thesis. It calculates and plots the pressure fields of the forward or backward propagation steps of TR in a half-space environment using a simple source. The TRM can be a circular or square layout, aperture can be varied in terms of radians, the source to field ratio (SFR) is calculated in each iteration and stored in 'data'. Each iteration plots the pressure field. The pressure fields are vectorized which speeds up computation time significantly.

```
1 %%%%%%%%%%%%%%%%%%%%%%%%%%%%%%%%%%%%%%%%%%%%%%%%%%%%%%%%%%%%%%%%%%%%%%%%%%
2 %DESCRIPTION: FORWARD/BACKWARD TIME REVERSAL PROPAGATION
3 %AUTHOR: BLAINE HARKER (blaineharker at gmail dot com)
4 %INPUT:
5 %OUTPUT:
6 %SUBROUTINES:
7 %PROJECT: Simple time reversal in a half-space environment
8 %DATE: 05/09/2012
9 %%%%%%%%%%%%%%%%%%%%%%%%%%%%%%%%%%%%%%%%%%%%%%%%%%%%%%%%%%%%%%%%%%%%%%%%%%
10 %
11 % Calculates and plots the pressure fields of the forward or backward
12 % propagation steps of TR in a half-space environment using a simple
```

```

13 % source. The TRM can be a circular or square layout, aperture can be
14 % varied in terms of radians, the source to field ratio (SFR) is calculated
15 % in each iteration and stored in 'data'. Each iteration plots the pressure
16 % field. The pressure fields are vectorized which speeds up computation time
17 % significantly.
18 %
19 %%%%%%%%%%%%%%%%%%%%%%%%%%%%%%%%%%%%%%%%%%%%%%%%%%%%%%%%%%%%%%%%%%%%%%%%%%
20
21 % INITIALIZE PARAMETERS
22 clear; close all;
23 tic
24 maxpoints=50;
25 param=[2,1.5,1,1/2,1/3,1/4,1/6,1/12]; %Different aperture sizes (radians/pi)
26
27 f=9000; %Frequency
28 A=1; %Amplitude
29 c=343; %Speed of Sound
30 T=1/f; %Period
31 w=2*pi*f; %Angular Frequency
32 k=w/c; %Wavenumber
33 lambda=c/f; %Wavelength
34 h=lambda/50; %Field Spacing
35 lam=lambda/h; %Points in one wavelength
36 t=0; %time (held constant for these plots)
37
38 %%%%%%%%%%%%%%%%%%%%%%%%%%%%%%%%%%%%%%%%%%%%%%%%%%%%%%%%%%%%%%%%%%%%%%%%%%
39 % Set default plot values for matlab session
40 set(0,'DefaultAxesFontName','Times New Roman');
41 set(0,'DefaultTextFontName','Times New Roman');
42 set(0,'DefaultAxesFontSize',14); % for a paper, this should be 18
43 set(0,'DefaultTextFontSize',14);
44 set(0,'DefaultAxesFontWeight','demi')
45 set(0,'DefaultTextFontWeight','demi')
46 set(0,'DefaultAxesLineWidth',2); % for paper consider 2
47 set(0,'DefaultLineLineWidth',2);
48 set(0,'DefaultLineMarkerSize',8); % for paper consider 8
49
50 xt=-13*lambda:h:13*lambda; %Field of interest
51 yt=-13*lambda:h:13*lambda; %Field Size adjusted for field being averaged
52 fsizex=length(xt);
53 fsizey=length(yt);
54
55 % INITIALIZE VARIABLES
56 Maxqual = zeros(maxpoints,2); %Collects SFR for specific aperture
57
58 %'data' stores 'Maxqual' info before changing aperture size. It contains
59 % data ( aperture run , SFR(TRM element #), 2 ) or
60 % data ( aperture run , TRM Elements, 1 )
61 data=zeros( length( param ), maxpoints ,2);
62
63 trm.shape = 'square'; %TRM Shape 'circle' or 'square'
64 direction = 'backward'; %'forward' or 'backward' propagation step
65 for ww=1:length(param) %loop through aperture sizes
66     ang=param(ww); %current aperture angle (radians)
67     for points=1:maxpoints %loop through number TRM elements in TRM
68
69         [x y ~]=meshgrid(xt,yt,1:points); % Initialize pressure field
70
71         z=1.5*lambda;
72         xso=0; %Original Point Source
73         yso=-12*lambda; % (0,0) corresponds to xso=0,yso=-12*lambda
74         zs=1.5*lambda; %Source / TRM height above ground
75

```

```

76 % TRM Element Location
77 lxc=xso; %X-Position center of Line Array
78 ly=yso; %Y-Position center of Line Array
79 lz=zs; %Z-Position center of Line Array
80
81 % Arc Array Field
82 r=12*lambda; %Radius of TRM from its geometric center
83 theta=ang*pi; %aperture angle (radians)
84 cent=r+ly; %Y Distance from (lxc,ly) to circle center
85
86 % Initialize arrays to calculate TRM element positions
87 pa=zeros(length(points),3);
88 pa2=zeros(length(points),3);
89 pasquare=zeros(length(points),3);
90 for i=1:points
91     if points == 1
92         pa(i,:)=[r,(i-1)*theta/(points)-(theta+pi/2) lz];
93     elseif ang == 2
94         pa(i,:)=[r,(i-1)*theta/(points)-(theta+pi/2) lz];
95     else
96         pa(i,:)=[r,(i-1)*theta/(points-1)-(theta+pi/2) lz];
97     end
98
99     if strcmp(trm.shape,'circle')
100         % Calculate TRM element positions for a circular TRM
101         pa2(i,:)=[lxc+pa(i,1)*cos(pa(i,2)),...
102                 cent+pa(i,1)*sin(pa(i,2)),pa(i,3)];
103     elseif strcmp(trm.shape,'square')
104         % Calculate TRM element positions for a circular TRM
105         %Divide up angles into eight groups
106         % (zero is south and + angles move ccwise)
107         if pa(i,2)>= -5*pi/2 && pa(i,2)<-9*pi/4 % 0-45
108             pasquare(i,:)=[lxc+r*sqrt(1/(sin(pa(i,2))^2)-1),...
109                             cent-r, pa(i,3)];
110         elseif pa(i,2)>= -9*pi/4 && pa(i,2)<-2*pi % 45-90
111             pasquare(i,:)=[lxc+r,...
112                             cent-r*sqrt(1/(cos(pa(i,2))^2)-1), pa(i,3)];
113         elseif pa(i,2)>=-2*pi && pa(i,2) < -7*pi/4 % 90-135
114             pasquare(i,:)=[lxc+r,...
115                             cent+r*sqrt(1/(cos(pa(i,2))^2)-1), pa(i,3)];
116         elseif pa(i,2)>=-7*pi/4 && pa(i,2) < -3*pi/2 % 135-180
117             pasquare(i,:)=[lxc+r*sqrt(1/(sin(pa(i,2))^2)-1),...
118                             cent+r, pa(i,3)];
119         elseif pa(i,2)>= -3*pi/2 && pa(i,2) < -5*pi/4 % 180-225
120             pasquare(i,:)=[lxc-r*sqrt(1/(sin(pa(i,2))^2)-1),...
121                             cent+r, pa(i,3)];
122         elseif pa(i,2)>=-5*pi/4 && pa(i,2) < -pi %225-270
123             pasquare(i,:)=[lxc-r,...
124                             cent+r*sqrt(1/(cos(pa(i,2))^2)-1), pa(i,3)];
125         elseif pa(i,2)>=-pi && pa(i,2) < -3*pi/4 %270-315
126             pasquare(i,:)=[lxc-r,...
127                             cent-r*sqrt(1/(cos(pa(i,2))^2)-1), pa(i,3)];
128         else %315 - 360
129             pasquare(i,:)=[lxc-r*sqrt(1/(cos(pa(i,2)-pi/2)^2)-1),...
130                             cent-r, pa(i,3)];
131         end
132     else
133         error('Abort: Wrong TRM Shape')
134     end
135 end
136 if strcmp(trm.shape,'square')
137     %Individual X,Y,Z components of each Element
138     x0=pasquare(:,1);y0=pasquare(:,2);z0=pasquare(:,3);

```

```

139     elseif strcmp(trm.shape, 'circle')
140         %Individual X,Y,Z components of each Element
141         x0=pa2(:,1);y0=pa2(:,2);z0=pa2(:,3);
142     end
143
144     % Vectorized TRM elements
145     [~,~,x0grid]=meshgrid(1:fsizex,1:fsizey,x0);
146     [~,~,y0grid]=meshgrid(1:fsizex,1:fsizey,y0);
147     [~,~,z0grid]=meshgrid(1:fsizex,1:fsizey,z0);
148     % data2=zeros(201,201,1,4);
149
150     %There is code to calculate the SFR as the source is moved at
151     % different locations in the field. Default position (center)
152     % is x = 1, y = 51;
153     %for this project the source is centered relative to the TRM
154     for xx=1%26:201 % 15 wavelengths at 1/10 lambda increments
155         for yy=51%51:201
156             xs=(xx-1)/10*lambda; %Current source location (x)
157             ys=cent;%(yy-1)/10*lambda; %Current source location (y)
158
159             %find source indices on the field
160             xfieldp = find(xt>=xs,1,'first');
161             xfieldn = find(xt<xs,1,'last');
162             yfieldp = find(yt>=ys,1,'first');
163             yfieldn = find(yt<ys,1,'last');
164             if abs(xt(xfieldp)-xs)>abs(xt(xfieldn)-xs)
165                 cpx = xfieldn;
166             else cpx=xfieldp;
167             end
168             if abs(yt(yfieldp)-ys)>abs(yt(yfieldn)-ys)
169                 cpy = yfieldn;
170             else cpy=yfieldp;
171             end
172
173             %Define indices of the bounds where the field near the
174             % source will be averaged.
175             boxLength = 5.0*lam;
176             fl=cpx - boxLength/2;
177             fr=cpx + boxLength/2;
178             ft=cpy + boxLength/2;
179             fb=cpy - boxLength/2;
180             cpos=[ft-cpy, fr-cpx];
181
182             %Define indices of the bounds that will be discluded from the
183             % field average (source location).
184             sboxlength = .5*lam;
185             sourcel=cpx - round(sboxlength/2);
186             sourcer=cpx + round(sboxlength/2);
187             sourceb=cpy - round(sboxlength/2);
188             sourcect=cpy + round(sboxlength/2);
189
190             %Forward propagation step amplitude (B) and phase(theta)
191             % for direct and reflected paths
192             B1=A./sqrt((x0grid-xs).^2+(y0grid-ys).^2+(zs-z0grid).^2);
193             B2=A./sqrt((x0grid-xs).^2+(y0grid-ys).^2+(zs+z0grid).^2);
194             theta1=k*sqrt((x0grid-xs).^2+(y0grid-ys).^2+(zs-z0grid).^2);
195             theta2=k*sqrt((x0grid-xs).^2+(y0grid-ys).^2+(zs+z0grid).^2);
196
197             %Calculate the field of the forward propagation step
198             [xfor yfor]=meshgrid(xt,yt);
199             zfor = z0grid(1,1,1);
200             ps1 = A./sqrt((xfor-xs).^2+(yfor-ys).^2+(zs-zfor).^2).*...
201                 exp(-1i*(k*sqrt((xfor-xs).^2+(yfor-ys).^2+(zs-zfor).^2)));

```

```

202     ps1 = ps1 + A./sqrt((xfor-xs).^2+(yfor-ys).^2+(zs+zfor).^2).*...
203         exp(-1i*(k*sqrt((xfor-xs).^2+(yfor-ys).^2+(zs+zfor).^2)));
204
205     %Remove infinite field points
206     for i=1:length(yt)
207         for ii=1:length(xt)
208             if isinf(ps1(i,ii))
209                 ps1(i,ii)=0;
210             end
211         end
212     end
213
214     %Backward propagation step partial pressure fields for:
215     % direct,direct / reflected,direct / direct,reflected /
216     % and reflected / reflected arrival paths
217     ps1prime=B1./sqrt((x-x0grid).^2+(y-y0grid).^2+...
218         (z-z0grid).^2).*exp(-1i*(w*t-k*sqrt((x-x0grid).^2+...
219         (y-y0grid).^2+(z-z0grid).^2)+theta1));
220     ps1prime=ps1prime+B2./sqrt((x-x0grid).^2+(y-y0grid).^2+...
221         (z-z0grid).^2).*exp(-1i*(w*t-k*sqrt((x-x0grid).^2+...
222         (y-y0grid).^2+(z-z0grid).^2)+theta2));
223     ps1prime=ps1prime+B1./sqrt((x-x0grid).^2+(y-y0grid).^2+...
224         (z+z0grid).^2).*exp(-1i*(w*t-k*sqrt((x-x0grid).^2+...
225         (y-y0grid).^2+(z+z0grid).^2)+theta1));
226     ps1prime=ps1prime+B2./sqrt((x-x0grid).^2+(y-y0grid).^2+...
227         (z+z0grid).^2).*exp(-1i*(w*t-k*sqrt((x-x0grid).^2+...
228         (y-y0grid).^2+(z+z0grid).^2)+theta2));
229
230     %Plot either forward or backward propagation step
231     if strcmp(direction,'forward')
232         field = ps1;
233     elseif strcmp(direction,'backward')
234         field=ps1prime;
235     end
236     clear ps1prime B1 B2 theta1 theta2;
237
238     %Sum vectorized portions of the field
239     field=sum(field,3);
240
241     %Remove infinite field points
242     for i=1:length(yt)
243         for ii=1:length(xt)
244             if isinf(field(i,ii))
245                 field(i,ii)=0;
246             end
247         end
248     end
249
250     % Calculate amplitude at source location
251     centermax=abs(field(cpy,cpx));
252
253
254     % Initialize temporary field
255     fieldA=zeros(length(field(:,1)),length(field(1,:)));
256     % Field of only source location area
257     fieldA(sourceb:sourcet,sourcel:sourcer)=...
258         field(sourceb:sourcet,sourcel:sourcer);
259     % Initialize temporary field
260     fieldB = field - fieldA;
261     %Take field near source (box) minus the pressure at source
262     ftot=fieldB(fb:ft,fl:fr);
263     %Average field value
264     fieldavg=mean(mean(abs(ftot)));

```

```

265         % Source to field ratio (SFR)
266         ratio=centermax / fieldavg;
267
268         clc; display(ww); disp(points);%display(xx); display(yy);
269     end
270 end
271
272 %Store TRM element number and SFR for iteration
273 Maxqual(points,:)= [points ratio];
274
275 %%%%%%%%%%%%%%%%%%%%%%%%%%%%%%%%%%%%%%%%%%%%%%%%%%%%%%%%%%%%%%%%%%%%%%%%%
276 % Plotting
277
278 % %Plot Source and Field
279 convNewPlot = h/h;
280 ppoints=(max(max(real(field)))+20).*ones(length(x0));
281
282 % Calculate Region of certainty outline
283 xp=[xs/lambda-2.5*convNewPlot,xs/lambda-2.5*convNewPlot,...
284     xs/lambda+2.5*convNewPlot,xs/lambda+2.5*convNewPlot];
285 yp=[ys/lambda-2.5*convNewPlot,ys/lambda+2.5*convNewPlot,...
286     ys/lambda+2.5*convNewPlot,ys/lambda-2.5*convNewPlot];
287 zp=[max(max(real(field))) max(max(real(field)))+20,...
288     max(max(real(field))) max(max(real(field)))+20];
289
290 % Create the Absolute Field Using the same metrics
291 figure('Visible','on')
292 hold on
293 % surf(xt/lambda,yt/lambda,abs(abs(field))); %Plot pressure mag.
294 surf(xt/lambda,yt/lambda,real(field)); %Plot real pressure mag.
295 shading interp
296
297 % TRM POSITION
298 plot3(x0./lambda,y0./lambda,ppoints,...
299     'ko','markersize',8,'markerfacecolor','w')
300
301 % Region of certainty outline
302 line(xp(1:2),yp(1:2),zp(1:2),'LineWidth',2,'Color','k');
303 line(xp(2:3),yp(2:3),zp(2:3),'LineWidth',2,'Color','k');
304 line(xp(3:4),yp(3:4),zp(3:4),'LineWidth',2,'Color','k');
305 line([xp(4),xp(1)],[yp(4) yp(1)],[zp(4) zp(1)],...
306     'LineWidth',2,'Color','k');
307
308 axis image;
309 colorbar
310 xlabel('X Position (\lambda)'); %Set to 18 if main, 24 if subfigure
311 ylabel('Y Position (\lambda)');
312
313 caxis([-max(max(abs(ftot))) max(max(abs(ftot)))]);
314 box on
315 hold off
316
317 end
318 % Save Maxqual data for aperture iteration
319 data(ww,,:)=Maxqual;
320 end
321 toc
322
323 % [EOF]

```



```

43
44 % LINE ARRAY CONSTANT ANGLE / CONSTANT INTERELEMENT SPACING (BOOLEAN)
45 % (FOR CONSTANT ANGLE - CHOOSE 1 , FOR CONSTANT SPACING - CHOOSE 2)
46 % (NOTE - IF Trm.AngAperture >= pi IT WILL BE MODIFIED TO A QUASI-INF LINE)
47 Trm.FixLineAngle = 1;
48
49 % LINE ARRAY ELEMENT SPACING
50 % (FOR LINE ARRAY USE ONLY)
51 Trm.LineArraySpacing = 5.00;    % [Wavelengths]
52
53 % FREQUENCY
54 f = 9000; % [Hz]
55
56 % SOURCE SHIFT
57 % (define the location where the source will be placed (relative to the
58 % TRM Center. If a vector is given, seperate results are given for each
59 % position)
60 Source.x = 0;%-20:4/3:20;          % [WAVELENGTHS]
61 Source.y = 0;%-20:4/3:20;          % ["]
62 Source.z = 0;%[0 -1.5 -3.0 -4.5 -(1/(343/9000))]; % ["] (SINGLE VALUE)
63
64 % Z-POSITION OF FIELD OF INTEREST
65 % (if length(Source.z) > 1 this value is replaced with z = zs )
66 z = Trm.Center.z;
67
68 % ITERATE THROUGH ONE OF INITIAL PARAMETERS (OTHER THAN SOURCE SHIFT)
69 % (STRING) (EG 'Trm.AngAperture')
70 Trm.iterPar = '';    % TYPE VARIABLE NAME OR LEAVE BLANK
71
72 % QUALITY FACTOR MEASUREMENT BOOLEANS
73 FieldAverage.GetQ = 1;    % Collect Quality Factor Information
74 FieldAverage.GetPeak = 1; % Collect Source to Peak Ratio Information
75
76 % FIELD BOX SHAPE
77 % (SHAPE OF THE AREA WHERE FIELD WILL BE AVERAGED)(STRING)
78 FieldAverage.Shape = 'square';    % 'circle' or 'square'
79
80 % FIELD BOX SIDE TO CENTER DISTANCE
81 % (L/2 FOR FIELD SQUARE, R FOR FIELD CIRCLE)
82 FieldAverage.SetBoxSize = 1;    % Sets the box size relative to 9 kHz
83 FieldAverage.BoxSide = 5.0;    % [Wavelengths]
84
85 % DISCLUDE 1/4 WAVELENGTH BOX AROUND SOURCE IN FIELD AVERAGE? (BOOLEAN)
86 FieldAverage.MinusSource = 1;
87
88 % FIGURE BOOLEANS
89 % (Choose 1 for True, 0 for False)
90 fig.draw = 1; % Plot the field
91 fig.visual = 1; % Display plot on screen (0 creates an invisible plot)
92 fig.iter = 0; % Plot in iteration mode (closes figures at the end of loop)
93 fig.iterX = 0; % Plot in Xtreme iteration mode (creates only field needed)
94
95 % SAVE BOOLEANS
96 % (Choose 1 to save data, 0 to supress saving data)
97 saveIt.data = 0;
98 saveIt.fig = 0;
99 saveIt.logfile = 0;
100
101 % LOGFILE COMMENTS
102 logme.my_comments = '[Enter Comments Here]';
103
104 % SAVE FILE LOCATION
105 saveIt.file = 'Location_to_save_data';

```

```

106 saveIt.date = 'Current_Data';
107 saveIt.ID = 'Desired_ID';
108
109 % COMPLETION NOTIFICATION BOOLEANS
110 % (Choose 1 to notify, 0 to suppress notification)
111 done.email = 0;
112 done.text = 0;
113 done.sound = 0;
114
115 %__SET FIGURE PROPERTIES FOR REMAINDER OF MATLAB SESSION__%
116 set(0, 'DefaultAxesFontName', 'Arial');
117 set(0, 'DefaultAxesFontSize', 14);
118 set(0, 'DefaultAxesFontWeight', 'demi');
119 set(0, 'DefaultAxesLineWidth', 1.5);
120 set(0, 'DefaultLineLineWidth', 2);
121 set(0, 'DefaultLineMarkerSize', 8);
122 set(0, 'DefaultFigurePosition', get(0, 'ScreenSize'));
123
124 %%%%%%%%%%%%%%%%%%%%%%%%%%%%%%%%%%%%%%%%%%%%%%%%%%%%%%%%%%%%%%%%%%%%%%%%%%
125 %%%%%%%%%%%%%%%%%%%%%%%%%%%%%%%%%%%%%%%%%%%%%%%%%%%%%%%%%%%%%%%%%%%%%%%%%%
126 % EXECUTE INITIAL SEQUENCES
127
128 % MAKE DIRECTORY
129 if saveIt.data || saveIt.logfile || saveIt.fig
130
131     % CREATE DATE FOLDER
132     if exist([saveIt.file, '/', saveIt.date], 'file') == 0
133         mkdir([saveIt.file, '/', saveIt.date]);
134     end
135
136     % CREATE ID FOLDER
137     if exist([saveIt.file, '/', saveIt.date, '/', saveIt.ID], 'file') == 0
138         mkdir([saveIt.file, '/', saveIt.date, '/', saveIt.ID]);
139     end
140 end
141
142 if saveIt.logfile
143
144     % TURN DIARY ON
145     diary([saveIt.file, '/', saveIt.date, '/', saveIt.ID, '/', saveIt.ID, ...
146         '_diary.out'])
147     disp('Diary is Recording');
148 end
149
150 % CHECK IF ID ALREADY EXISTS
151 if exist([saveIt.file, '/', saveIt.date, '/', saveIt.ID, '/', saveIt.ID, '.mat'], ...
152     'file') == 2 && (saveIt.data || saveIt.fig || saveIt.logfile)
153     cont = input('The ID Being Used Already Exists. Continue ? y/n: ', 's');
154     if strcmp(cont, 'n') || strcmp(cont, 'N')
155         return
156     end
157     clear cont
158 end
159
160 %%%%%%%%%%%%%%%%%%%%%%%%%%%%%%%%%%%%%%%%%%%%%%%%%%%%%%%%%%%%%%%%%%%%%%%%%%
161 % MANY ITERATION INITIALIZATIONS
162
163 % PREALLOCATE ARRAYS AND INITIALIZE DUMMY VARIABLES
164 if isempty(Trm.iterPar)
165     Trm.iterPar = 'f';
166 end
167 eval(['iterPar = ', Trm.iterPar, ';']);
168 figNote = 0;

```

```

169 ttime = zeros(length(iterPar),...
170     length(Source.x)*length(Source.y)*length(Source.z));
171 loc_quality = zeros(length(iterPar),length(Source.x),length(Source.y));
172 peak_quality = zeros(length(iterPar),length(Source.x),length(Source.y));
173 progress = 0;
174
175 % ITERATE THROUGH AN INITIAL PARAMETER IF DESIGNATED
176 for nn = 1:length(iterPar)
177     % RUN THROUGH EACH OF THE PARAMETERS INDIVIDUALLY
178     if nn == 1
179         eval(['iterAll = ',Trm.iterPar, ';']);
180     end
181     eval(['Trm.iterPar, ' = ', 'iterAll(',num2str(nn), ');']);
182
183     % NOTE OF MULTIPLE ITERATIONS
184     if length(iterPar) > 1
185         disp(['Iterating through parameter ',Trm.iterPar, ' ',...
186             num2str(length(iterPar)), ' Times:']);
187         disp(['Current Iteration : ',num2str(nn), ' / ',...
188             num2str(length(iterPar))]);
189     end
190
191     % FIGURE SAVE WARNING
192     if length(iterPar) > 1 && figNote < 1 && saveIt.fig
193         disp('Note: Figures will only be saved for the first iteration');
194         cont = input('Continue ? y/n : ', 's');
195         if strcmp(cont, 'n') || strcmp(cont, 'N')
196             return
197         end
198         figNote = 1;
199     end
200
201     %%%%%%%%%%%%%%%%%%%%%%%%%%%%%%%%%%%%%%%%%%%%%%%%%%%%%%%%%%%%%%%%%%%%%%%%%%%
202     % DEFINE SOURCE AND FIELD OF INTEREST
203
204     % SIMPLE SOURCE
205     A=1; %Amplitude
206     c=343; %Speed of Sound
207     T=1/f; %Period
208     w=2*pi*f; %Angular Frequency
209     k=w/c; %Wavenumber
210     lambda=c/f; %Wavelength
211     t = 0; %Time
212
213     % FIELD PARAMETERS
214     fieldvar.side = 2.0; %Length of Field Edges [m]
215     fieldvar.h = lambda/50; %Field Spacing [m]
216
217     % XTREME ITERATION MODE (SMALLER FIELDS)
218     if fig.iterX
219
220         % CHECK IF USING PC (SUPERCOMPUTER SKIPS THIS)
221         if ispc
222
223             % MEMORY ERROR CHECK
224             [mem.userv mem.sysv] = memory;
225             mem.smallfield = (2*FieldAverage.BoxSide*lambda/fieldvar.h)^2;
226             mem.req = mem.smallfield*Trm.Num*8 * (5) + mem.smallfield*16 + ...
227                 768e6 + 2e9;
228             if mem.req > mem.sysv.PhysicalMemory.Available
229                 ME = MException('VerifyInput:Limit',...
230                     'Not Enough Available Physical Memory');
231                 throw(ME);

```

```

232         end
233         clear mem
234     end
235
236 else
237
238     % FIELD RANGES
239     xt = Trm.Center.x-fieldvar.side/2:fieldvar.h:Trm.Center.x +...
240         fieldvar.side/2;
241     yt = Trm.Center.y-fieldvar.side/2:fieldvar.h:Trm.Center.y +...
242         fieldvar.side/2;
243     zt = Trm.Center.z;
244
245     % CHECK IF USING PC (SUPERCOMPUTER SKIPS THIS)
246     if ispc
247
248         % MEMORY ERROR CHECK (For the Dell Workstation Used, about
249         % 40GB Memory limit)
250         [mem.userv mem.sysv] = memory;
251         mem.req = length(xt)*length(yt)*Trm.Num*8 * (5) +...
252             length(xt)*length(xt)*16 + 768e6 + 2e9;
253         if mem.req > mem.sysv.PhysicalMemory.Available
254             ME = MException('VerifyInput:Limit',...
255                 'Not Enough Available Physical Memory');
256             throw(ME);
257         end
258         clear mem
259     end
260
261     % DEFINE VECTORIZED FIELD
262     fieldvar.size.x = length(xt);
263     fieldvar.size.y = length(yt);
264     [x y ~] = meshgrid(xt, yt, 1:Trm.Num);
265
266 end
267
268 % WAVELENGTH -> FIELD SPACING CONVERSION
269 fieldvar.conv = lambda / fieldvar.h;
270
271 % CONVERT BOX SIDE: [WAVELENGTHS] -> [M]
272 if FieldAverage.SetBoxSize
273     FieldAverage.BoxSideM = FieldAverage.BoxSide*(343/9000);
274 else
275     FieldAverage.BoxSideM = FieldAverage.BoxSide*lambda;
276 end
277
278 %%%%%%%%%%%%%%%%%%%%%%%%%%%%%%%%%%%%%%%%%%%%%%%%%%%%%%%%%%%%%%%%%%%%%%%%%%%
279 % DEFINE TIME REVERSAL MIRROR
280
281 % CIRCLE OR MODIFIED SQUARE TRM CONSTRUCTION
282 if strcmp(Trm.Type, 'circle') || strcmp(Trm.Type, 'modified_square')
283
284     setup.pa = zeros(Trm.Num,3);
285     setup.pa2 = zeros(Trm.Num,3);
286
287     % LOOP THROUGH TRM ELEMENTS
288     for i = 1:Trm.Num
289         if Trm.Type == 1
290             setup.pa(i,:) = [Trm.Dist, (i-1)*Trm.AngAperture/Trm.Num-...
291                 (Trm.AngAperture+pi/2), ...
292                 Trm.Center.z];
293             elseif Trm.AngAperture == 2*pi
294                 setup.pa(i,:) = [Trm.Dist, (i-1)*Trm.AngAperture/Trm.Num-...

```

```

295         (Trm.AngAperture+pi/2),Trm.Center.z];
296     else
297         setup.pa(i,:)=[Trm.Dist,...
298             (i-1)*Trm.AngAperture/(Trm.Num-1)-...
299             (Trm.AngAperture+pi/2),Trm.Center.z];
300     end
301
302     % SQUARE TRM
303     if strcmp(Trm.Type,'modified_square')
304
305         setup.papasquare=zeros(Trm.Num,3);
306
307         %DIVIDE ANGLES INTO 8 GROUPS
308         % (zero is south and + angles move ccwise)
309         if setup.pa(i,2)>= -5*pi/2 && setup.pa(i,2)<-9*pi/4 % 0-45
310             setup.pasquare(i,:)=[...
311                 Trm.Center.x +...
312                 Trm.Dist*sqrt(1/(sin(setup.pa(i,2))^2)-1),...
313                 Trm.Center.y-Trm.Dist,...
314                 setup.pa(i,3)];
315         elseif setup.pa(i,2)>= -9*pi/4 && setup.pa(i,2)<-2*pi % 45-90
316             setup.pasquare(i,:)=[...
317                 Trm.Center.x+Trm.Dist, Trm.Center.y-...
318                 Trm.Dist*sqrt(1/(cos(setup.pa(i,2))^2)-1),...
319                 setup.pa(i,3)];
320         elseif setup.pa(i,2)>=-2*pi && setup.pa(i,2) < -7*pi/4 % 90-135
321             setup.pasquare(i,:)=[...
322                 Trm.Center.x+Trm.Dist, Trm.Center.y+...
323                 Trm.Dist*sqrt(1/(cos(setup.pa(i,2))^2)-1),...
324                 setup.pa(i,3)];
325         elseif setup.pa(i,2)>=-7*pi/4 && setup.pa(i,2) < -3*pi/2 % 135-180
326             setup.pasquare(i,:)=[Trm.Center.x+...
327                 Trm.Dist*sqrt(1/(sin(setup.pa(i,2))^2)-1),...
328                 Trm.Center.y+Trm.Dist,...
329                 setup.pa(i,3)];
330         elseif setup.pa(i,2)>= -3*pi/2 && setup.pa(i,2)< -5*pi/4 % 180-225
331             setup.pasquare(i,:)=[...
332                 Trm.Center.x-Trm.Dist*...
333                 sqrt(1/(sin(setup.pa(i,2))^2)-1),Trm.Center.y+...
334                 Trm.Dist,setup.pa(i,3)];
335         elseif setup.pa(i,2)>=-5*pi/4 && setup.pa(i,2) < -pi %225-270
336             setup.pasquare(i,:)=[Trm.Center.x-Trm.Dist,...
337                 Trm.Center.y+Trm.Dist*...
338                 sqrt(1/(cos(setup.pa(i,2))^2)-1),setup.pa(i,3)];
339         elseif setup.pa(i,2)>=-pi && setup.pa(i,2) < -3*pi/4 %270-315
340             setup.pasquare(i,:)=[Trm.Center.x-Trm.Dist,...
341                 Trm.Center.y-Trm.Dist*...
342                 sqrt(1/(cos(setup.pa(i,2))^2)-1),setup.pa(i,3)];
343         else %315 - 360
344             setup.pasquare(i,:)=[Trm.Center.x-Trm.Dist*...
345                 sqrt(1/(cos(setup.pa(i,2)-pi/2)^2)-1),...
346                 Trm.Center.y-Trm.Dist,setup.pa(i,3)];
347         end
348     else
349         % CIRCLE TRM
350         setup.pa2(i,:)=[...
351             Trm.Center.x + setup.pa(i,1)*cos(setup.pa(i,2)),...
352             Trm.Center.y + setup.pa(i,1)*sin(setup.pa(i,2)),...
353             setup.pa(i,3)];
354     end
355
356     %Individual X,Y,Z components of each Element
357     if strcmp(Trm.Type,'modified_square')

```

```

358         x0=setup.pasquare(:,1);
359         y0=setup.pasquare(:,2);
360         z0=setup.pasquare(:,3);
361     else
362         x0=setup.pa2(:,1);
363         y0=setup.pa2(:,2);
364         z0=setup.pa2(:,3);
365     end
366 end
367
368 % LINE ARRAY CONSTRUCTION
369 elseif strcmp(Trm.Type, 'line')
370
371     if Trm.FixLineAngle
372         % CONSTANT ANGLE LINE TRM
373
374         % CHECK THAT ANGULAR APERTURE IS LESS THAN 180 DEGREES
375         if Trm.AngAperture >= pi
376
377             % LINE ARRAY WILL BE QUASI-INFINITE
378             setup.lineAngle = pi - .01;
379         else
380             setup.lineAngle = Trm.AngAperture;
381         end
382
383         % DEFINE ARRAY LENGTH [m]
384         setup.ArrayLength = 2 * Trm.Dist * tan(setup.lineAngle/2);
385
386         % REDEFINE ELEMENT SPACING [WAVELENGTHS]
387         Trm.LineArraySpacing = setup.ArrayLength / (Trm.Num - 1)...
388             / lambda;
389
390     else
391         % CONSTANT INTERELEMENT SPACING
392
393         % DEFINE ARRAY LENGTH [m]
394         setup.ArrayLength = (Trm.Num - 1) * Trm.LineArraySpacing * lambda;
395
396     end
397
398     for i = 1:Trm.Num
399         % DEFINE LINE ARRAY ALONG X DIRECTION
400         setup.pa(i,:) = [...
401             (Trm.Center.x - setup.ArrayLength/2) +...
402             (i-1)*Trm.LineArraySpacing*lambda, Trm.Center.y - Trm.Dist, ...
403             Trm.Center.z];
404     end
405
406     x0 = setup.pa(:,1);
407     y0 = setup.pa(:,2);
408     z0 = setup.pa(:,3);
409 else
410     ME = MException('VerifyInput:Undefined', 'TRM Type is not recognized');
411     throw(ME);
412 end
413 clear setup
414
415 if ~fig.iterX
416
417     % VECTORIZE TRM ELEMENTS FOR FASTER COMPUTATION
418     [~,~,x0grid]=meshgrid(1:fieldvar.size.x,1:fieldvar.size.y,x0);
419     [~,~,y0grid]=meshgrid(1:fieldvar.size.x,1:fieldvar.size.y,y0);
420     [~,~,z0grid]=meshgrid(1:fieldvar.size.x,1:fieldvar.size.y,z0);

```

```

421
422     end
423     %%%%%%%%%%%%%%%%%%%%%%%%%%%%%%%%%%%%%%%%%%%%%%%%%%%%%%%%%%%%%%%%%%%%%%%%%%
424     % RUN THROUGH TEST
425
426     % LOOP THROUGH SOURCE POSITIONS: X-POSITION
427     for xx=1:length(Source.x)
428
429         %LOOP THROUGH SOURCE POSITIONS: Y-POSITIONS
430         for yy= 1:length(Source.y)
431
432             % TIMER AND COUNTER
433             tic
434             progress = progress + 1;
435
436             % CURRENT SOURCE POSITION
437             xs = Source.x(xx) * lambda + Trm.Center.x;
438             ys = Source.y(yy) * lambda + Trm.Center.y;
439
440             % CHECK IF ITERATING THROUGH Z-POSITION
441             if length(Source.z) > 1
442                 zs = Source.z(nn) * lambda + Trm.Center.z;
443                 z = zs;
444             else
445                 zs = Source.z * lambda + Trm.Center.z;
446             end
447
448             % XTREME ITERATION MODE
449             if fig.iterX
450
451                 xt = xs - FieldAverage.BoxSideM:fieldvar.h:xs + ...
452                     FieldAverage.BoxSideM;
453                 yt = ys - FieldAverage.BoxSideM:fieldvar.h:ys + ...
454                     FieldAverage.BoxSideM;
455                 zt = Trm.Center.z;
456
457                 % DEFINE VECTORIZED FIELD
458                 fieldvar.size.x = length(xt);
459                 fieldvar.size.y = length(yt);
460                 [x y ~] = meshgrid(xt, yt, 1:Trm.Num);
461
462                 % VECTORIZIZE TRM ELEMENTS FOR FASTER COMPUTATION
463                 [~,~,x0grid]=meshgrid(1:fieldvar.size.x,...
464                                     1:fieldvar.size.y,x0);
465                 [~,~,y0grid]=meshgrid(1:fieldvar.size.x,...
466                                     1:fieldvar.size.y,y0);
467                 [~,~,z0grid]=meshgrid(1:fieldvar.size.x,...
468                                     1:fieldvar.size.y,z0);
469
470             end
471
472             % AMPLITUDES AND PHASING FROM FORWARD PROPAGATION
473             % (1 = DIRECT, 2 = REFLECTED)
474             B1=A./sqrt((x0grid-xs).^2+(y0grid-ys).^2+(zs-z0grid).^2);
475             B2=A./sqrt((x0grid-xs).^2+(y0grid-ys).^2+(zs+z0grid).^2);
476             theta1=k*sqrt((x0grid-xs).^2+(y0grid-ys).^2+(zs-z0grid).^2);
477             theta2=k*sqrt((x0grid-xs).^2+(y0grid-ys).^2+(zs+z0grid).^2);
478
479             % BACKWARD PROPAGATION
480             % (DIR/REF TAKE DIRECT PATH, DIR/REF TAKE REFLECTED PATH)
481             ps1prime=B1./sqrt((x-x0grid).^2+(y-y0grid).^2+(z-z0grid).^2).*...
482                 exp(-1i*(w*t-k*sqrt((x-x0grid).^2+(y-y0grid).^2+...
483                     (z-z0grid).^2)+theta1));

```

```

484     ps1prime=ps1prime+B2./sqrt((x-x0grid).^2+(y-y0grid).^2+...
485         (z-z0grid).^2).*...
486     exp(-li*(w*t-k*sqrt((x-x0grid).^2+(y-y0grid).^2+...
487         (z-z0grid).^2)+theta2));
488 ps1prime=ps1prime+B1./sqrt((x-x0grid).^2+(y-y0grid).^2+...
489     (z+z0grid).^2).*...
490     exp(-li*(w*t-k*sqrt((x-x0grid).^2+(y-y0grid).^2+...
491         (z+z0grid).^2)+theta1));
492 ps1prime=ps1prime+B2./sqrt((x-x0grid).^2+(y-y0grid).^2+...
493     (z+z0grid).^2).*...
494     exp(-li*(w*t-k*sqrt((x-x0grid).^2+(y-y0grid).^2+...
495         (z+z0grid).^2)+theta2));
496
497 % COLLAPSE FIELD TOGETHER AND CLEAR TEMPORARY VARIABLES
498 field=sum(ps1prime,3);
499 clear ps1prime B1 B2 theta1 theta2;
500
501 % REMOVE UNBOUNDED VALUES
502 for i=1:length(yt)
503     for ii=1:length(xt)
504         if isinf(field(i,ii))
505             field(i,ii)=0;
506         end
507     end
508 end
509 clear i ii
510
511 %%%%%%%%%%%%%%%%%%%%%%%%%%%%%%%%%%%%%%%%%%%%%%%%%%%%%%%%%%%%%%%%%%%%%%%%%%%
512 % QUALITY FACTOR MEASUREMENTS
513
514 % LOCATE SOURCE POSITION ON FIELD
515 xfp = find(xt >= xs,1,'first');
516 xfn = find(xt < xs,1,'last');
517 yfp = find(yt >= ys,1,'first');
518 yfn = find(yt < ys,1,'last');
519 if abs(xt(xfp)-xs) > abs(xt(xfn)-xs)
520     cpx = xfn;
521 else cpx=xfp;
522 end
523 if abs(yt(yfp)-ys)>abs(yt(yfn)-ys)
524     cpy = yfn;
525 else cpy=yfp;
526 end
527 clear xfp xfn yfp yfn
528
529 % AMPLITUDE AT SOURCE POSITION
530 centermax = abs(field(cpy,cpx));
531
532 if FieldAverage.GetQ
533
534     % DETERMINE FIELD TYPE TO CREATE
535     if strcmp(FieldAverage.Shape,'square')
536         % SQUARE FIELD AVERAGE
537
538         if ~fig.iterX
539
540             %ERROR CHECKING
541             if abs(xs - FieldAverage.BoxSideM) > abs(xt(1))...
542                 || abs(xs + FieldAverage.BoxSideM) > abs(xt(end))...
543                 || abs(ys - FieldAverage.BoxSideM) > abs(yt(1)) ...
544                 || abs(ys + FieldAverage.BoxSideM) > abs(yt(end))
545                 ME = MException('VerifyInput:Limit',...
546                     'Field is not large enough for averaging');

```

```

547         throw(ME);
548     end
549 end
550
551 % FIND FIELD SIDES [INDEXED POINTS]
552 fl = find(xt >= xs - FieldAverage.BoxSideM,1, 'first');
553 fr = find(xt <= xs + FieldAverage.BoxSideM,1, 'last');
554 fb = find(yt >= ys - FieldAverage.BoxSideM,1, 'first');
555 ft = find(yt <= ys + FieldAverage.BoxSideM,1, 'last');
556
557 if FieldAverage.MinusSource
558
559     % FIND SOURCE SIDES [INDEXED POINTS]
560     sbox = .25*lambda;
561     sl=cpx - round(sbox * fieldvar.conv);
562     sr=cpx + round(sbox * fieldvar.conv);
563     sb=cpy - round(sbox * fieldvar.conv);
564     st=cpy + round(sbox * fieldvar.conv);
565
566     % ZERO POINTS ABOUT SOURCE
567     Fieldtemp = field;
568     Fieldtemp(sb:st, sl:sr) = 0;
569
570     % AVERAGE FIELD WITHOUT SOURCE
571     FieldAverage.Avg = ...
572         mean(mean(abs((Fieldtemp(fb:ft, fl:fr)))));
573     clear Fieldtemp sl sr sb st
574
575 else
576
577     % AVERAGE FIELD WITH SOURCE
578     FieldAverage.Avg = ...
579         mean(mean(abs((field(fb:ft, fl:fr)))));
580
581 end
582
583 clear fl fr fb ft
584
585 elseif strcmp(FieldAverage.Shape, 'circle')
586     % CIRCLE FIELD AVERAGE
587
588     if ~fig.iterX
589
590         %ERROR CHECKING
591         if abs(xs - FieldAverage.BoxSideM) > abs(xt(1))...
592             || abs(xs + FieldAverage.BoxSideM) > abs(xt(end))...
593             || abs(ys - FieldAverage.BoxSideM) > abs(yt(1)) ...
594             || abs(ys + FieldAverage.BoxSideM) > abs(yt(end))
595             ME = MException('VerifyInput:Limit', ...
596                 'Field is not large enough for averaging');
597             throw(ME);
598         end
599     end
600
601     % INITIALIZE TEMPORARY ITERATORS
602     count = 0;
603     fieldavgtot = 0;
604
605     % LOOP THROUGH EACH POINT ON THE FIELD
606     for i = 1:length(field(:,1))
607         for ii = 1:length(field(1,:))
608
609             % DISTANCE FROM SOURCE TO FIELD POINT

```

```

610         % [INDEXED POINTS]
611         rDist = sqrt((cpx-ii)^2+(cpy-i)^2);
612
613         % CIRCLE RADIUS [INDEXED POINTS]
614         circleR = FieldAverage.BoxSideM / lambda *...
615             fieldvar.conv;
616
617         % SOURCE IS WITHIN CIRCLE AND NOT WITHIN
618         % 1/4 WAVELENGTH OF SOURCE
619         if rDist <= circleR && rDist > 0.25*fieldvar.conv
620             fieldavgtot = fieldavgtot + abs(field(i,ii));
621             count = count + 1;
622         end
623     end
624 end
625 if count == 0
626     FieldAverage.Avg = 0;
627 else
628     FieldAverage.Avg = real(fieldavgtot/count);
629 end
630 clear i ii rDist count fieldavgtot circleR;
631
632 else
633     ME = MException('VerifyInput:Undefined',...
634         'Field Average Shape is not recognized');
635     throw(ME)
636 end
637
638 % GIVE LOCALIZATION QUALITY RATIO
639 loc_quality (nn,xx,yy) = centermax / FieldAverage.Avg;
640
641 end
642
643 % SOURCE TO PEAK RATIO
644 if FieldAverage.GetPeak
645
646     % DEFINE TEMPORARY FIELD
647     Fieldtemp = field;
648
649     % FIND FIELD SIDES [INDEXED POINTS]
650     fl = find(xt >= xs - FieldAverage.BoxSideM,1,'first');
651     fr = find(xt <= xs + FieldAverage.BoxSideM,1,'last');
652     fb = find(yt >= ys - FieldAverage.BoxSideM,1,'first');
653     ft = find(yt <= ys + FieldAverage.BoxSideM,1,'last');
654
655     % DISCLUDE AMPLITUDES FROM SOURCE POSITION
656     % FIND SOURCE SIDES [INDEXED POINTS]
657     sbox = .25; % [WAVELENGTHS]
658     sl=cpx - round(sbox * fieldvar.conv);
659     sr=cpx + round(sbox * fieldvar.conv);
660     sb=cpy - round(sbox * fieldvar.conv);
661     st=cpy + round(sbox * fieldvar.conv);
662
663     % ZERO POINTS ABOUT SOURCE
664     Fieldtemp(sb:st, sl:sr) = 0;
665
666     % DEFINE FIELD WHERE PEAK WILL BE LOCATED
667     fieldPeak = Fieldtemp(fb:ft, fl:fr);
668
669     % LOCATE PEAK AMPLITUDE ( MAX( |AVERAGE BOX| ) )
670     [px py] = find(real(fieldPeak) == ...
671         max(max(real(fieldPeak))),1,'first');
672

```

```

673         % GIVE SOURCE TO NEXT PEAK RATIO
674         peak_quality (nn,xx,yy) = centermax / real(fieldPeak(px,py));
675
676         % CLEAR TEMPORARY VARIABLES
677         clear Fieldtemp fieldPeak sl sr sb st fl fr fb ft sbox ...
678             px py
679
680     end
681
682     %%%%%%%%%%%%%%%%%%%%%%%%%%%%%%%%%%%%%%%%%%%%%%%%%%%%%%%%%%%%%%%%%%%%%%%%%%
683     % PLOTTING
684
685     % WHETHER TO PLOT DATA
686     if fig.draw
687
688         % PLOT IS VISIBLE OR NOT
689         if fig.visual
690             figure
691         else
692             figure('Visible','off')
693         end
694
695         % PLOT USING PCOLOR
696         pcolor(xt,yt,real(field));
697         hold on
698
699         % FIGURE PROPERTIES
700         shading interp
701
702         % ADD CONTOUR LINES
703         [C,hc] = contour(xt,yt,abs(field),10,'k',...
704             'LevelList',centermax/2);
705
706         % ADD POINTS FOR THE TRM ELEMENTS
707         if ~(Trm.AngAperture >= pi && strcmp(Trm.Type,'line'))
708             ppoints=(max(max(real(field)))+20).*ones(length(x0));
709             plot3(x0,y0,ppoints,'ko','markersize',6,'markerfacecolor','k')
710         end
711
712         % ADD A POINT AT THE SOURCE
713         % plot3(xs,ys,max(max(max(real(field))))+20,'ko',...
714         % 'markersize',6,'markerfacecolor','k');
715
716         % ADD A POINT AT THE TRM CENTER
717         % plot3(Trm.Center.x,Trm.Center.y,...
718         % max(max(max(real(field))))+20,...
719         % 'bx','markersize',6,'markerfacecolor','k')
720
721         if strcmp(FieldAverage.Shape,'square')
722
723             % ADD A SQUARE OVER WHICH THE FIELD IS AVERAGED
724             xp=[xs-FieldAverage.BoxSideM,xs-FieldAverage.BoxSideM,...
725                 xs+FieldAverage.BoxSideM,xs+FieldAverage.BoxSideM];
726             yp=[ys-FieldAverage.BoxSideM,ys+FieldAverage.BoxSideM,...
727                 ys+FieldAverage.BoxSideM,ys-FieldAverage.BoxSideM];
728             zp=[max(max(real(field))), max(max(real(field))),...
729                 max(max(real(field))) max(max(real(field)))];
730             line(xp(1:2),yp(1:2),zp(1:2),'LineWidth',2,'Color','k');
731             line(xp(2:3),yp(2:3),zp(2:3),'LineWidth',2,'Color','k');
732             line(xp(3:4),yp(3:4),zp(3:4),'LineWidth',2,'Color','k');
733             line([xp(4),xp(1)],[yp(4) yp(1)],[zp(4) zp(1)],...
734                 'LineWidth',2,'Color','k');
735

```

```

736
737         elseif strcmp(FieldAverage.Shape, 'circle')
738
739             % ADD A CIRCLE OVER WHICH THE FIELD IS AVERAGED
740             J=circle([Trm.Center.x,Trm.Center.y,...
741                 max(max(real(field))+200),...
742                 FieldAverage.BoxSideM,1000,'k-');
743             set(J,'LineWidth',2);
744
745         end
746
747         % OTHER FIGURE PROPERTIES
748         axis image;
749         colorbar
750         xlabel('X Position (m)','FontSize',18);
751         ylabel('Y Position (m)','FontSize',18);
752         if FieldAverage.GetQ || FieldAverage.GetPeak
753             if FieldAverage.GetPeak
754                 title(['...
755                     %'Source / Field = ',num2str(loc_quality(nn,xx,yy)),...
756                     'Source / Peak = ',num2str(peak_quality(nn,xx,yy))],...
757                     'FontSize',16);
758             else
759                 title(['Source vs Field = ',...
760                     num2str(loc_quality(nn,xx,yy))], 'FontSize',16);
761             end
762         end
763         caxis([-centermax centermax])
764         set(gca,'fontsize',16);
765         hold off
766
767
768         %%%%%%%%%%%%%%%%%%%%%%%%%%%%%%%%%%%%%%%%%%%%%%%%%%%%%%%%%%%%%%%%%%%%%%%%%%%
769         % SAVE DATA AND NOTIFY OF COMPLETION
770
771         % SAVE FIGURE
772         if saveIt.fig
773             if nn == 1
774                 print('-dpng',[saveIt.file, '/', saveIt.date, '/', ...
775                     saveIt.ID, '/', saveIt.ID, '_Fig_', ...
776                     num2str(xx), '_', num2str(yy)]);
777             end
778         end
779
780         % ITERATION MODE
781         if fig.iter
782             close all;
783         end
784
785     end
786
787     % DISPLAY PROGRESS
788     ttime(nn, progress) = toc;
789     disp(['Source Position:(', num2str(xs), ', ', num2str(ys), ', ', ...
790         num2str(zs), ') Finished in ', num2str(toc), ...
791         ' sec - Progress: ', ...
792         num2str(progress), ' / ', num2str(length(Source.x)*...
793         length(Source.y)*length(Source.z))]);
794 end
795 end
796
797 % HOLD ON TO TRM VALUES IF IT CHANGES
798 if length(iterPar) > 1

```

```

799         if length(Trm.iterPar) > 3
800             if strcmp(Trm.iterPar(1:4), 'Trm. ')
801                 eval(['x0tot.N', num2str(nn), ' = x0; ']);
802                 eval(['y0tot.N', num2str(nn), ' = y0; ']);
803                 eval(['z0tot.N', num2str(nn), ' = z0; ']);
804             end
805         end
806     end
807 end
808 end
809
810 % SAVE VARIABLES
811 if saveIt.data && (FieldAverage.GetQ || FieldAverage.GetPeak)
812     if FieldAverage.GetQ
813         loc_quality = squeeze(loc_quality);
814         save([saveIt.file, '/', saveIt.date, '/', saveIt.ID, '/', saveIt.ID], ...,
815             'loc_quality');
816     end
817     if FieldAverage.GetPeak
818         peak_quality = squeeze(peak_quality);
819         save([saveIt.file, '/', saveIt.date, '/', saveIt.ID, '/', saveIt.ID, 'P'], ...,
820             'peak_quality');
821     end
822 end
823
824 % CREATE LOG FILE
825 if saveIt.logfile
826
827     % RETURN PARAMETER ITERATOR TO INITIAL STATE
828     if length(iterPar) > 1
829         eval(['Trm.iterPar, ' = ', 'iterAll; ']);
830     end
831
832     logme.date = ['Processing Date: ', datestr(now)];
833     logme.mfile = mfilename;
834
835     % SAVE TRM BASED ON ITERATION PARAMETER
836     if length(Trm.iterPar) > 3 && strcmp(Trm.iterPar(1:4), 'Trm. ')
837         logme.Parameters.x0 = x0tot;
838         logme.Parameters.y0 = y0tot;
839         logme.Parameters.z0 = z0tot;
840     else
841         logme.Parameters.x0 = x0;
842         logme.Parameters.y0 = y0;
843         logme.Parameters.z0 = z0;
844     end
845
846     logme.Parameters.f = f;
847     logme.Parameters.lambda = lambda;
848     logme.Source = Source;
849     logme.Trm = Trm;
850     if FieldAverage.GetQ
851         logme.FieldAverage = FieldAverage;
852     end
853     save([saveIt.file, '/', saveIt.date, '/', saveIt.ID, '/', saveIt.ID, ...,
854         '_logfile'], 'logme');
855
856     % TURN DIARY OFF
857     diary off
858 end
859
860 % CLEAN UP AND FINISH

```

```
862
863 tottime = sum(sum(ttime));
864 fprintf('\n\t Total Time Elapsed: %f seconds\n', tottime);
865
866 clearvars
867 fprintf('\t\t-\t-\t-\t-\n\t\tProgram Complete\n\t\t-\t-\t-\t-\n');
868
869 % [EOF]
```

Bibliography

- ¹ M. Fink, “Time-reversal of ultrasonic fields. 1. basic principles”, *Ieee Trans. Ultra. Ferro. Freq. Ctrl.* **39**, 555–566 (1992).
- ² M. Fink, “Time reversed acoustics”, *Phys. Today* **50**, 34–40 (1997).
- ³ A. Parvulescu and C. Clay, “Reproducibility of signal transmissions in the ocean”, *Radio Elec. Eng.* **29**, 223 –228 (1965).
- ⁴ B. E. Anderson, M. Griffa, C. Larmat, T. J. Ulrich, and P. A. Johnson, “Time reversal”, *Acoust. Today* **4**, 5–16 (2008).
- ⁵ J.-L. Thomas, F. Wu, and M. Fink, “Time reversal focusing applied to lithotripsy”, *Ultra. Imag.* **18**, 106–121 (1996).
- ⁶ C. S. Larmat, R. A. Guyer, and P. A. Johnson, “Time-reversal methods in geophysics”, *Phys. Today* **63**, 31–35 (2010).
- ⁷ G. S. O’Brien, I. Lokmer, L. De Barros, C. J. Bean, G. Saccorotti, J. P. Metaxian, and D. Patane, “Time reverse location of seismic long-period events recorded on mt etna”, *Geophys. J. Int.* **184**, 452–462 (2011).
- ⁸ T. J. Ulrich, P. A. Johnson, and R. A. Guyer, “Interaction dynamics of elastic waves with a complex nonlinear scatterer through the use of a time reversal mirror”, *Phys. Rev. Lett.* **98**, 104301 (2007).
- ⁹ T. J. Ulrich, A. M. Sutin, T. Claytor, P. Papin, P. Y. Le Bas, and J. A. TenCate, “The time reversed elastic nonlinearity diagnostic applied to evaluation of diffusion bonds”, *Appl. Phys. Lett.* **93**, 151914 (2008).
- ¹⁰ C. Prada, S. Manneville, D. Spoliansky, and M. Fink, “Decomposition of the time reversal operator: Detection and selective focusing on two scatterers”, *J. Acoust. Soc. Am.* **99**, 2067–2076 (1996).
- ¹¹ B. E. Anderson, M. Griffa, P.-Y. L. Bas, T. J. Ulrich, and P. A. Johnson, “Experimental implementation of reverse time migration for nondestructive evaluation applications”, *J. Acoust. Soc. Am.* **129**, EL8–EL14 (2011).

- ¹² A. Sutin, B. Libbey, L. Fillinger, and A. Sarvazyan, “Wideband nonlinear time reversal seismo-acoustic method for landmine detection”, *J. Acoust. Soc. Am.* **125**, 1906–1910 (2009).
- ¹³ A. Song and M. Badiey, “Time reversal acoustic communication for multiband transmission”, *J. Acoust. Soc. Am.* **131**, EL283–EL288 (2012).
- ¹⁴ B. E. Anderson, R. A. Guyer, T. J. Ulrich, and P. A. Johnson, “Time reversal of continuous-wave, steady-state signals in elastic media”, *AIP* **94**, 111908 (2009).
- ¹⁵ M. Fink, D. Cassereau, A. Derode, C. Prada, P. Roux, and M. Tanter, “Time-reversed acoustics”, *Rep. on Prog. Phys.* **63**, 1933–1995 (2000).
- ¹⁶ J. Kraus and R. Marhefka, *Antennas for all applications*, 3rd edition (McGraw-Hill, Woodbury, NY) (2002).
- ¹⁷ M. Fink, “Time-reversal mirrors”, *J. Phys. D: Appl. Phys.* **26**, 1333 (1993).
- ¹⁸ C. S. Larmat, R. A. Guyer, and P. A. Johnson, “Tremor source location using time reversal: Selecting the appropriate imaging field”, *Geophys. Res. Lett.* **36**, L22304 (2009).
- ¹⁹ B. E. Anderson, M. Griffa, T. J. Ulrich, and P. A. Johnson, “Time reversal reconstruction of finite sized sources in elastic media”, *J. Acoust. Soc. Am.* **130**, EL219–EL225 (2011).
- ²⁰ M. Tanter, J. L. Thomas, F. Coulouvrat, and M. Fink, “Breaking of time reversal invariance in nonlinear acoustics”, *Phys. Rev. E* **64**, 016602 (2001).
- ²¹ K. B. Cunningham, M. F. Hamilton, A. P. Brysev, and L. M. Krutyansky, “Time-reversed sound beams of finite amplitude”, *J. Acoust. Soc. Am.* **109**, 2668–2674 (2001).
- ²² K. L. Gee, A. A. Atchley, L. E. Falco, M. R. Shepherd, L. S. Ukeiley, B. J. Jansen, and J. M. Seiner, “Bicoherence analysis of model-scale jet noise”, *J. Acoust. Soc. Am.* **128**, EL211–EL216 (2010).
- ²³ D. of Veterans Affairs, “Veterans benefits administration annual benefits report fiscal year 2010”, 5.
- ²⁴ T. R. Board, “Effects of aircraft noise: Research update on selected topics”, **2008**.
- ²⁵ A. T. Wall, K. L. Gee, M. D. Gardner, T. B. Neilsen, and M. M. James, “Near-field acoustical holography applied to high-performance jet aircraft noise”, *Proc. Meet. Acoust.* **9**, 040009 (2011).
- ²⁶ S. H. Swift and K. L. Gee, “Examining the use of a time-varying loudness algorithm for quantifying characteristics of nonlinearly propagated noise (I)”, *J. Acoust. Soc. Am.* **129**, 2753–2756 (2011).

-
- ²⁷ J. Morgan, T. B. Neilsen, K. L. Gee, A. T. Wall, and M. M. James, “Simple-source model of high-power jet aircraft noise”, submitted to *Noise Control Eng. J.* (2011).
- ²⁸ S. F. Wu and N. Zhu, “Locating arbitrarily time-dependent sound sources in three dimensional space in real time”, *J. Acoust. Soc. Am.* **128**, 728–739 (2010).
- ²⁹ Q. Zhang, H. Abeida, M. Xue, W. Rowe, and J. Li, “Fast implementation of sparse iterative covariance-based estimation for source localization”, *J. Acoust. Soc. Am.* **131**, 1249–1259 (2012).
- ³⁰ K. L. Gee, V. W. Sparrow, M. M. James, J. M. Downing, C. M. Hobbs, T. B. Gabrielson, and A. A. Atchley, “The role of nonlinear effects in the propagation of noise from high-power jet aircraft”, *J. Acoust. Soc. Am.* **123**, 4082–4093 (2008).